Hindawi
Wireless Communications and Mobile Computing
Volume 2022, Article ID 4258113, 22 pages
https://doi.org/10.1155/2022/4258113

Research Article

Throughput Maximization for Wireless Powered Buffer-Aided Successive Relaying Networks

Yong Liu,[1] Qingchun Chen,[2] and Lin X. Cai[3]

[1]*South China Normal University, China*
[2]*Guangzhou University, Guangzhou, China*
[3]*Illinois Institute of Technology, Chicago, USA*

Correspondence should be addressed to Qingchun Chen; qcchen@gzhu.edu.cn

Received 30 October 2021; Revised 13 March 2022; Accepted 18 March 2022; Published 13 May 2022

Academic Editor: Quoc-Tuan Vien

In this paper, we consider a wireless powered cooperative network, where two energy-constrained buffer-aided relays harvest energy from the source to assist the information delivery to the destination. To improve the spectral efficiency, a wireless powered successive relaying (WPSR) protocol is proposed to allow both relays to receive the information from the source and forward the buffered data to the destination, taking into consideration of the inter-relay-interference (IRI). We first reveal the impact of data buffers and energy storages at the relays by the achievable throughput comparison of the WPSR scheduling schemes with and without considering data buffers and energy storages. Our analysis validates the great potential of the buffer-and-forward data transmission and the harvest-store-use energy management strategies. Then, the network throughput is maximized via adaptive time and power allocation subject to the stability constraints of data buffers and energy buffers, and an adaptive wireless powered buffer-aided successive relaying (WPBSR) scheduling scheme is proposed. The proposed scheme approaches the optimal throughput of the wireless powered successive relaying network with bounded delay and finite length of data and energy buffers. Numerical results validate the analysis and noticeable spectral efficiency gain.

1. Introduction

Radio frequency (RF) signal can not only be utilized for wireless information transfer (WIT) but also employed for energy harvesting to power devices, namely, wireless energy transfer (WET) [1]. Thus, simultaneous wireless information and power transfer (SWIPT) framework is exploited in [2–4], where the received signal is divided into two separated parts for concurrent WIT and WET in either time or power domain, i.e., time-switching (TS) and power splitting (PS). Afterward, how to explore SWIPT into diverse networks has attracted many research efforts to realize the sustainable wireless networking [5]. As buffer-aided communication [6, 7] enables data to be firstly stored and then adaptively transmitted according to the underlying channel conditions, it has shown its great potential to either reduce energy expenditure [8] or enlarge network throughput [9, 10]. Thus, how to jointly exploit the advantage of both SWIPT and buffer-aided communication is critical to achieve the energy-sustainable and efficient communication systems.

As cooperative communication can effectively improve network throughput and enlarge the coverage, it is integrated with the SWIPT in wireless powered cooperative communication networks (WPCNs), which has been extensively studied in [11–20]. For a WPCN, the ergodic capacity of TS-based and PS-based relaying protocols was analyzed in [11–13] and then the TS and PS parameters were optimized in [14, 15] to maximize the network throughput. Meanwhile, the relay selection and scheduling policies for a wireless powered multirelay network were investigated in [16–20]. While the potential of buffer-aided communication has not been fully exploited in all these works.

Basically, in buffer-aided relaying networks, the transmission link can be activated according to both the instantaneous link quality and the buffer status to realize a higher network throughput through adaptive link selection [10,

21] and relay selection [22–24]. When exploiting buffer-aided communication strategy into wireless powered cooperative networks, the network throughput can be maximized via the adaptive link/relay selection [25–28] and time/power allocation [29–31]. Nonetheless, these works mainly investigate half-duplex relaying (HDR), which leads to some loss of spectral efficiency [32].

Full-duplex relaying (FDR) [33–37] and successive relaying (SR) [38–51] are two representative techniques to further improve the spectral efficiency. Since sophisticated full-duplex circuits and self-interference suppression technology are no longer needed, SR provides us with an effective solution that simultaneously selects two relays to receive information from the source and forward the message to the destination, such that it can be interpreted as a virtual FDR. The achievable rate and adaptive resource allocation of a SR network were investigated in [38–40] without considering energy harvesting capability. Instead, the network throughput of an energy harvesting (EH) based two-relay network was maximized in [42] via adaptively selecting the broadcast, multiaccess, and successive relaying transmission modes. An adaptive two-path successive relaying (TPSR) protocol was proposed in [43] for a wireless powered two-relay network, in which the relay selection was alternatively utilized if TSPR fails. The aforementioned research works aim to either analyze or optimize the achieved performance and do not attempt to exploit the great benefit of the buffer-aided communication strategy. For a buffer-aided successive relaying network, the transmission policy design and resource scheduling were studied in [44–49] without energy harvesting. In [50], the relays of an EH-based SR network were provisioned with data buffers and energy storages, and the network throughput was maximized in the absence of inter-relay-interference (IRI). In addition, the energy is assumed to be harvested from the surrounding environment (e.g., solar or wind), which is usually sporadic and intermittent. On the contrary, controllable RF-based energy harvesting [1] seems more attractive for designing wireless-powered communication systems with strict QoS requirements. In [51], the achieved performance (i.e., outage probability and achievable rate) of a buffer-aided EH-based SR network was analyzed, wherein the energy storage and adaptive resource management were not incorporated to maximize network throughput. All these observations motivate us to unveil the effect of both data buffers and energy storages and investigate the maximum achievable network throughput for a wireless powered buffer-aided SR network via adaptive resource scheduling.

In this paper, a wireless powered successive relaying network is studied, in which two energy-constrained relays are charged via the transmitted signals from the source. A wireless powered successive relaying (WPSR) protocol is firstly incorporated, where two relays are charged in WET phases and then alternatively selected in a successive relaying manner to simultaneously receive information from the source and forward data to destination within WIT phases. In order to unveil the effect of data buffers and energy storages, we then analyze and compare the achievable throughputs of WPSR schemes with and without data buffers and energy storages. It is validated that the data buffer at the relays can introduce throughput gain. This is because the buffer-and-forward data management policy results the end-to-end throughput equal to the minimum expected rate of both hops, instead of the expectation of the minimum instantaneous rate. In addition, the energy storage can enlarge the achievable throughput via harvest-store-use energy policy. Leveraging the analysis, we then focus on the maximum achievable network throughput and formulate a throughput maximization problem under the constraints of data buffer stability and energy sustainability. By employing Lyapunov optimization framework, an adaptive wireless powered buffer-aided successive relaying (WPBSR) scheme is proposed to adaptively allocate transmit power and time slot to the weighted "best" transmission mode based on the instantaneous channel/buffer/energy state information (CSI, BSI, ESI). The performance analysis unveils that the achievable throughput of the WPBSR scheme can be arbitrarily close to the optimal performance with limited cost of delay, and finite lengths of data buffer and energy storage can be guaranteed. Finally, extensive simulation results validate the throughput gain of the proposed WPBSR scheme with data buffers and energy storages. The contributions of this paper are summarized as follows:

(i) By deploying data buffers and energy storages, the buffer-and-forward data management and harvest-store-use energy management policies can be exploited. On the basis, the achievable throughput of WPSR schemes is analyzed and compared to theoretically highlight the benefit of data buffers and energy storages

(ii) To maximize the achievable throughput, we propose an adaptive wireless powered buffer-aided successive relaying (WPBSR) scheme, which can adaptively allocate network resource (time, power) based on the CSI/BSI/ESI

(iii) Throughput gain of data buffers and energy storages is validated based on the extensive simulations, and the proposed WPBSR scheme can improve the network throughput with a cost of transmission delay

The remainder of the paper is organized as follows. The related works are presented in Section 2. The system model and the wireless powered successive relaying (WPSR) protocol are introduced in Section 3. The influence of data buffer and energy storage is analyzed in Section 4, and an adaptive WPBSR scheme is presented. Simulation results are provided in Section 5, followed by the conclusion in Section 6.

2. Related Work

Zhang et al. firstly proposed a simultaneous wireless information and power transfer (SWIPT) framework in [3], in which the time-switching (TS) and power-splitting (PS) protocols were utilized. Since then, the SWIPT has attracted many research attentions to realize the sustainable wireless communication systems [4, 5]. As an important application,

wireless powered cooperative communication (WPCN) can exploit the benefit of both cooperative communication and the RF energy harvesting technologies. The time-switching based relaying (TSR) and power-splitting based relaying (PSR) protocols were proposed in [11] to derive the ergodic capacity of a WPCN with an amplify-and-forward (AF) relay. When decode-and-forward (DF) mode was employed at the relay, the ergodic capacity was studied in [12]. As the harmful cochannel interference (CCI) could be utilized as energy source, the effect of CCI on the ergodic and outage capacity was investigated in [13]. In [14], the PS/TS coefficient was optimized to maximize the network throughput, in which the relay is assumed to be provisioned with rechargeable battery. For the multirelay WPCNs, the behavior of the energy storage at the relays was modeled as a two-state Markov chain in [16], such that the steady-state distribution and outage probability of relay selection scheme were analyzed. In [17], the multiple relays were simultaneously utilized according to the concept of distributed space-time coding. The beamforming design for multiantenna WPCN systems was investigated in [18, 19]. Relay selection and resource allocation schemes were studied in [20]. All these works aimed to either analyze or optimize the achieved performance of the SWIPT-based networks.

Recently, buffer-aided communication has shown its advantage of reducing energy expenditure [8] and improving network throughput [9, 10] with some cost of transmission delay. In [8], the transmission power was adaptively optimized based on the dynamic channel condition to minimize the energy consumption of a buffer-aided point-to-point system. Then, the buffer-aided communication was integrated with cooperative communication system, called buffer-aided relaying, and the performance analysis in [9] demonstrated that the buffer-aided relaying can improve the capacity of two-hop networks. With the assistance of data buffer, adaptive link selection strategy was exploited in [10, 21] where one link of both hops was adaptively activated based on the weighted instantaneous capacity. Then, the relay selection scheme was investigated for a buffer-aided multirelay network in [22–24]. Furthermore, wireless powered buffer-aided cooperative communication that can exploit the benefits of both buffer-aided relaying and RF energy harvesting technologies has been studied. In [25], the long-term network throughput of a wireless powered buffer-aided relaying system, where the relay charges the source via RF signals, was maximized via the adaptive link or mode selection. The achieved throughput for a buffer-aided wireless powered relay network was analyzed in [27]. In [28], the relay selection scheme was investigated for a multirelay network with considering data buffer and energy storage. The joint relay-and-mode selection scheme for a wireless powered buffer-aided multirelay network was addressed in [29] to maximize the network throughput. Then, the energy-efficient and secure transmission scheduling was studied in [30, 31], respectively. The above research works mainly investigated the throughput maximization of buffer-aided half-duplex relaying networks. While the half-duplex relaying may cause some loss in spectral efficiency [32].

To further improve the spectral efficiency, three emerging solutions were proposed, namely, half-duplex two-way relaying (HD-TWR), full-duplex relaying (FDR), and successive relaying (SR). HD-TWR was devised to support bidirectional information exchange between two terminals via one HD relay node. The achievable rate region of a buffer-aided HD-TWR network was analyzed in [52], and that of a wireless powered HD-TWR was studied in [53]. The full-duplex relay was enabled to receive and transmit over the same resource block, such that the network throughput of a buffer-aided FDR network was maximized in [36] via adaptive FD operation and power allocation, where the relay was enabled to receive and transmit over the same resource block. If the full-duplex relaying was employed with RF energy harvesting capability, the signal transmitted by the relay could also be reused for its energy harvesting, namely, the self-energy recycling [34]. The achievable rate and beamforming design for a multiantenna wireless powered FDR system were studied in [33, 35], respectively. In [37], the broadcasting and NOMA technique were integrated in a buffer-aided FDR network. Compared with the FDR, SR was a simple but efficient solution without the need of the sophisticated full-duplex circuit and self-interference cancellation technique. The achievable rate and resource allocation for SR networks were investigated in [38–41] without considering energy harvesting capability. In [42], the network throughput of an EH-based SR network was maximized via time and power allocation. The achieved performance of wireless powered two-relay network was investigated in [43]. Nonetheless, the data buffer at the relay was not exploited. In [44–49], the achieved performance and resource management for a buffer-aided SR network were investigated without considering energy harvesting capability. Under the complete interference cancellation assumption, the throughput maximization problem of an EH-based SR network without inter-relay-interference (IRI) was studied in [50] by considering both the data buffer and energy storage at relay. In addition, the nodes were assumed to harvest energy from surrounding environment like solar and wind, whose sporadic and intermittent nature might not fulfill the energy sustainable communication requirements. The achieved outage probability and achievable rate of a buffer-aided EH-based SR network were analyzed in [51], wherein the energy storage and adaptive resource management were not incorporated to maximize network throughput. Inspired by the recent research progress, we integrate the SR into wireless powered buffer-aided relaying network with practical inter-relay-interference (IRI) to improve the network throughput. Furthermore, we exploit and unveil the great potential of data buffer and energy storage at the relays and propose the adaptive wireless powered buffer-aided relaying scheme with adaptive time and power allocation.

3. Wireless Powered Successive Relaying Network

3.1. System Model. We study a wireless powered cooperative communication network as illustrated in Figure 1, in which one source $\mathcal{S}$ transmits data to the destination $\mathcal{D}$ with the

help of two energy-constrained relays $\mathscr{R}_1$ and $\mathscr{R}_2$. As the large transmission distance and channel blockage, there is no direct connection between $\mathscr{S}$ and $\mathscr{D}$, and their communication must be assisted with the intermediate relays. Both relays operate in half-duplex decode-and-forward (DF) mode and harvest energy from the source via the RF signals to forward the data to the destination. Define d_{Sk} and d_{kD} as the communication distances from $\mathscr{S}$ to $\mathscr{R}_k$[1] and from $\mathscr{R}_k$ to $\mathscr{D}$, respectively, and d_{12} is the distance between $\mathscr{R}_1$ and $\mathscr{R}_2$.

A time-slotted system is considered, where the transmission time is divided into time slots $t \in \{1, 2, \cdots, T\}$, and the duration of each slot is T_0 seconds. The channel coefficients are independent and slowly block fading, such that they remain unchanged in one-time slot but independently vary from one slot to another. Denote $h_{ij}(t) = \sqrt{L_{ij}}\tilde{h}_{ij}(t)$ as the channel gain of the link from node i to j in the time slot t, where L_{ij} and $\tilde{h}_{ij}(t)$ represent the large-scale and small-scale fading coefficient, respectively. $L_{ij} = L_0/(d_{ij}/d_0)^{\beta_{ij}}$, where L_0 is the reference path loss at the reference distance d_0, β_{ij} and d_{ij} denote the path loss exponent and the transmission distance, respectively. In addition, all involved links are assumed to be independent Rayleigh fading, and the average channel gain of the link between node i and node j is denoted as $\Omega_{ij} = \mathbb{E}[|h_{ij}(t)|^2]$. The transmit power of the source equals P_s, and those of both relays in time slot t are denoted as $P_1(t), P_2(t)$, respectively. σ^2 represents the background noise variance.

3.2. Wireless Powered Successive Relaying (WPSR) Protocol. To improve the spectral efficiency, successive relaying (SR) protocol is a promising approach for a multirelay system (Two relay scenario is investigated in this paper. Instead, the multirelay scenario can be similarly extended, where the relay selection need to be taken into consideration.), where two relays are selected within any time slot to receive the information from the source and to forward the previously received data to the destination, respectively. On the basis, we propose a wireless powered successive relaying (WPSR) protocol as illustrated in Figure 2, which consists of a wireless energy transfer (WET) phase and two wireless information transfer (WIT) phases. α is the fraction of time slot allocated for the dedicated WET, in which both relays simultaneously harvest energy from the RF signals transmitted by the source. The remaining $(1-\alpha)T$ time is used for WIT, in which the successive relaying is exploited. Similar to the conventional half-duplex relaying protocol, in the first $1/2(1-\alpha)T$, the relay $\mathscr{R}_1$ is supposed to receive data from $\mathscr{S}$ and the relay $\mathscr{R}_2$ is to forward its previously received data to $\mathscr{D}$ (WIT-I phase), while in the remaining $1/2(1-\alpha)T$, the relay $\mathscr{R}_2$ receives data from $\mathscr{S}$ and the relay $\mathscr{R}_1$ forwards its previously received data to the destination $\mathscr{D}$ (WIT-II phase). In the WET phase, the received energy signal at the relay $\mathscr{R}_k$ in time slot t is

$$Y_{k,e}(t) = \sqrt{P_s}h_{Sk}(t)s_e(t) + n_k(t), \tag{1}$$

where $s_e(t)$ is the energy signal transmitted by the source, and $n_k(t)$ represents the noise at $\mathscr{R}_k$. Therefore, the energy harvested by $\mathscr{R}_k$ in time slot t satisfies

$$e_k(t) = \alpha T \eta P_s |h_{Sk}(t)|^2, \tag{2}$$

where η is the energy conversion efficiency.

In the WIT phases, as the SR protocol is utilized, the received signal at $\mathscr{R}_k$ is

$$y_k(t) = \sqrt{P_s}h_{Sk}(t)s(t) + \sqrt{P_{k'}(t)}h_{kk'}(t)s_{k'}(t) + n_k(t), \tag{3}$$

where the first and second terms are the desired signal and the inter-relay interference (IRI), respectively. Thus, the corresponding signal-to-interference-plus-noise-ratio (SINR) is given by

$$\gamma_{Sk}(t) = \frac{P_s|h_{Sk}(t)|^2}{\sigma^2 + P_{k'}(t)|h_{kk'}(t)|^2}. \tag{4}$$

At the same time, the received signal at the destination $\mathscr{D}$ is

$$y_{k'D}(t) = \sqrt{P_{k'}(t)}h_{k'D}(t)x_{k'}(t) + n_D(t), \tag{5}$$

where $n_D(t)$ is the noise at $\mathscr{D}$. Thus, the signal-to-noise-ratio (SNR) of the link $\mathscr{R}_{k'}\mathscr{D}$ is

$$\gamma_{k'D}(t) = \frac{P_{k'}(t)|h_{k'D}(t)|^2}{\sigma^2}. \tag{6}$$

Likewise, the SINR of the link $\mathscr{S}\mathscr{R}_{k'}$ and the SNR of the link $\mathscr{R}_k\mathscr{D}$ can be obtained by exchanging k and k' in (4) and (6), respectively.

Given the SINR expressions, we can obtain the achieved transmission rates of all involved links. To this end, our goal is to maximize the achievable network throughput under the WPSR protocol.

4. Adaptive Wireless Powered Buffer-Aided Successive Relaying Scheme

In this section, to reveal the effect of both data buffers and energy storages, we analyze and compare the achieved throughput of WPSR scheduling schemes with and without data buffers and energy storages at the relays. Then, to maximize the network throughput, adaptive time and energy allocation are jointly optimized under the constraints of buffer stability and the energy sustainability, and an adaptive wireless powered buffer-aided successive relaying (WPBSR) scheduling scheme is proposed to adaptively allocate time slot and energy according to the dynamic CSI, BSI, and ESI. Finally, simulation results are presented to show that the achieved throughput of the proposed scheme can be arbitrarily close to the optimal scheduling scheme with limited cost of delay. In addition, the proposed scheme guarantees bounded data buffers and energy storages.

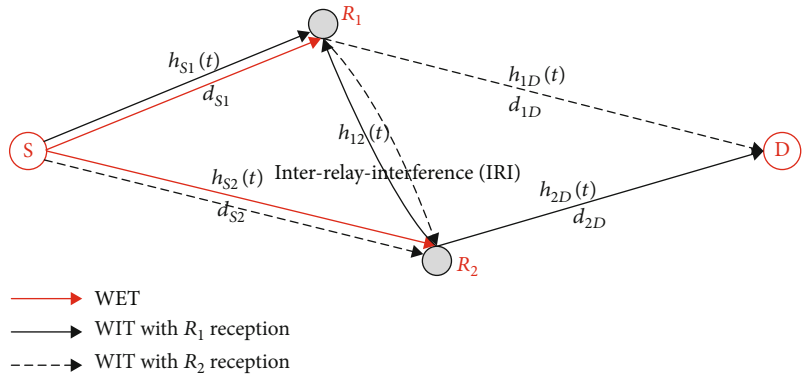

Figure 1: Wireless powered successive relaying network: one source, one destination, and two energy-constrained DF relays.

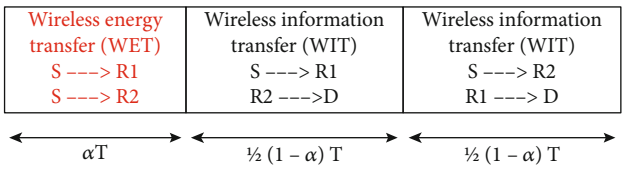

Figure 2: Time structure of wireless powered successive relaying (WPSR) protocol.

4.1. Throughput Analysis of WPSR. Our goal is to maximize network throughput under the WPSR protocol. As is stated in [9, 10], the data buffer at the relays can be exploited to improve the achieved performance of cooperative networks. Meanwhile, when the energy harvesting capability is deployed, the energy storage can be provisioned to efficiently utilize the harvested energy. Thus, to maximize the network throughput, we first analyze the network throughput of the WPSR scheduling scheme with and without data buffers and energy storages at the relays, such that the effects of both data buffers and energy storages are revealed.

4.1.1. WPSR Scheme without Data Buffers and Energy Storages. We firstly study the case that neither data buffers nor energy storages are provisioned. The relays first harvest energy and then use the collected energy for information transmission immediately, namely, harvest-use energy management strategy. Thus, the transmit power of $\mathscr{R}_k$ in the time slot t is $P_k(t) = 2\alpha/((1-\alpha)\eta P_s|h_{Sk}(t)|^2)$, and the SINR and SNR of $\mathscr{S}\mathscr{R}_k$ and $\mathscr{R}_k\mathscr{D}$ in (4) and (6) are rewritten as

$$\gamma_{Sk}(t) = \frac{P_s|h_{Sk}(t)|^2}{\sigma^2 + \kappa\eta P_s|h_{Sk'}(t)|^2|h_{kk'}(t)|^2}, \tag{7}$$

$$\gamma_{kD}(t) = \frac{\kappa\eta P_s|h_{Sk}(t)^2|h_{kD}(t)|^2}{\sigma^2}, \tag{8}$$

where $\kappa = 2\alpha/1-\alpha$ denotes the ratio between the WET time and the effective WIT time.

To analyze the achieved throughput, we need to obtain the statistical characteristics of the SNRs $\gamma_{Sk}(t)$, $\gamma_{kD}(t)$, e.g., the cumulative distribution functions (CDFs) and probability density functions (PDFs), in the following proposition.

Proposition 1. *When the harvest-use energy management strategy is utilized, namely, $P_k(t) = 2\alpha/(1-\alpha)\eta P_s|h_{Sk}(t)|^2$, the CDFs of $\gamma_{Sk}(t)$ and $\gamma_{kD}(t)$ in (7) and (8) are given by*

$$F_{\gamma_{Sk}}(\gamma) = 1 - \sqrt{\frac{\Omega_{Sk}}{\kappa\eta\Omega_{Sk'}\Omega_{kk'}\gamma}}\exp\left(-\frac{\sigma^2}{\Omega_{Sk}P_s}\gamma\right)\exp \cdot \left(\frac{\Omega_{Sk}}{2\kappa\eta\Omega_{Sk'}\Omega_{kk'}\gamma}\right)W_{-1/2,0}\left(\frac{\Omega_{Sk}}{\kappa\eta\Omega_{Sk'}\Omega_{kk'}\gamma}\right), \tag{9}$$

$$F_{\gamma_{kD}}(\gamma) = 1 - 2\sqrt{\frac{\sigma^2\gamma}{\kappa\eta P_s\Omega_{Sk}\Omega_{kD}}}K_1\left(2\sqrt{\frac{\sigma^2\gamma}{\kappa\eta P_s\Omega_{Sk}\Omega_{kD}}}\right), \tag{10}$$

where $K_n(x)$ and $W_{m,n}(x)$ are the n-th order modified Bessel function of the second kind and Whittaker functions [54], respectively. The corresponding PDFs are obtained by taking derivation of the CDFs with γ.

Proof. Please see appendix 7.

When data buffers are not exploited, the relays must firstly decode the data from the source and then immediately forward them to the destination. Thus, the end-to-end (E2E) SNR of the data transmission via two relays are the minimum SNR of two hops, i.e.,

$$\gamma_{S1D}(t) = \min\{\gamma_{S1}(t), \gamma_{1D}(t)\}, \tag{11}$$

$$\gamma_{S2D}(t) = \min\{\gamma_{S2}(t-1), \gamma_{2D}(t)\}. \tag{12}$$

Notice that, according to Figure 2, the E2E transmission via $\mathscr{R}_1$ is completed within one time slot, while the data transmission via $\mathscr{R}_2$ spans two successive time slots. Ergodic capacity that quantifies the ultimate reliable communication limit over the fading channel is derived by averaging the instantaneous capacity over all fading states, i.e., $C_{\text{non}} = \sum_{k=1,2}\mathbb{E}[1/2\log_2(1+\gamma_{SkD}(t))]$, where the subscript non implies no data buffer and energy storage at relays. Thus,

the achieved throughput is obtained by letting $\tau_{\text{non}} = (1-\alpha)C_{\text{non}}$, which is presented in the following lemma. □

Lemma 2. *When neither energy storage nor data buffer is provisioned at the relays, the achievable throughput of WPSR scheduling scheme is*

$$\begin{aligned}\tau_{non} &= \frac{1-\alpha}{2}\{\mathbb{E}[\log_2(1+\min\{\gamma_{S1}(t),\gamma_{1D}(t)\})] \\ &\quad + \mathbb{E}[\log_2(1+\min\{\gamma_{S2}(t-1),\gamma_{2D}(t)\})]\} \\ &= \frac{1-\alpha}{2}\sum_{k=1,2}\int_0^{+\infty}\log_2(1+\gamma)f_{\gamma_{SkD}}(\gamma)d\gamma.\end{aligned} \tag{13}$$

where the PDF $f_{\gamma_{SkD}}(\gamma)$ of the SNR $\gamma_{SkD}(t)$ is derived by taking derivation of the following CDF

$$\begin{aligned}F_{\gamma_{S1D}}(\gamma) = 1 - &\int_0^{+\infty}\frac{\gamma}{\Omega_{S1}P_s}\cdot\exp\left(-\frac{\gamma(x^2+\sigma^2)}{\Omega_{S1}P_s}-\frac{\sigma^2}{\kappa\eta P_s\Omega_{1D}(x+\sigma^2)}\right) \\ &\cdot\left[1-2\sqrt{\frac{x}{\kappa\eta P_s\Omega_{S1}\Omega_{12}}}K_1\left(2\sqrt{\frac{x}{\kappa\eta P_s\Omega_{S1}\Omega_{12}}}\right)\right]x,\end{aligned} \tag{14}$$

$$F_{\gamma_{S2D}}(\gamma) = 1 - \left[1-F_{\gamma_{S2}}(\gamma)\right]\left[1-F_{\gamma_{2D}}(\gamma)\right], \tag{15}$$

where the proof of $F_{\gamma_{S1D}}(\gamma)$ and $F_{\gamma_{S2D}}(\gamma)$ can be found in appendix 8.

4.1.2. WPSR with Only Data Buffers. We then investigate the case that the relays have data buffers but no energy storages. Hence, the relays can firstly store the decoded data into their buffers and then forward part or whole of the cached data to the destination, which means buffer-and-forward strategy is exploited. Accordingly, the ergodic capacity becomes the minimum ergodic capacity of two hops [9], i.e., $C_B = \sum_{k=1,2}\min\{\mathbb{E}[1/2\log_2(1+\gamma_{Sk}(t))],\mathbb{E}[1/2\log_2(1+\gamma_{kD}(t))]\}$. Noting that the practical rate from the relay to the destination is limited by the minimum of cached data and the instantaneous capacity. When the data buffer is filled in advance via caching procedure [55], i.e., caching part of popular contents in off peak time for the request in peak time, it can be guaranteed that the buffers always have enough data to be forwarded. As the instantaneous SNRs of all links are same with (7) and (8), the achievable throughput can be characterized by the following lemma.

Lemma 3. *When the data buffer at the relays is provisioned, the data management strategy becomes buffer-and-forward, in which the relay firstly stores the decoded data in its data buffer and then forwards part of the buffered data to the destination. Therefore, the achievable network throughput is*

$$\begin{aligned}\tau_B &= \frac{1-\alpha}{2}\sum_{k=1,2}\min\{\mathbb{E}[\log_2(1+\gamma_{Sk}(t))],\mathbb{E}[\log_2(1+\gamma_{kD}(t))]\} \\ &= \frac{1-\alpha}{2}\sum_{k=1,2}\min\left\{\int_0^{+\infty}\log_2(1+\gamma)f_{\gamma_{Sk}}(\gamma)d\gamma,\right. \\ &\quad \left.\cdot\int_0^{+\infty}\log_2(1+\gamma)f_{\gamma_{kD}}(\gamma)d\gamma\right\},\end{aligned} \tag{16}$$

where the PDFs $f_{\gamma_{Sk}}(\gamma)$ and $f_{\gamma_{kD}}(\gamma)$ are presented in Proposition 1.

By comparing the achievable throughput in (13) and (16), the WPSR scheme with data buffers outperforms that without data buffers as $\mathbb{E}[\min\{x,y\}] \le \min\{\mathbb{E}[x],\mathbb{E}[y]\}$, which indicates the data buffer can bring throughput gain.

4.1.3. WPSR with Only Energy Storages. When considering the energy storages at the relays, the energy management strategy becomes harvest-store-use, which means the relay can firstly collect energy to charge its energy storage and then consume part or whole stored energy for information delivery. Such that the energy allocation can be exploited. Average and optimal energy allocation are two typical strategies. In this subsection, we explore the average energy allocation to unveil the effect of energy storages. The optimal energy allocation will be studied through optimization method in the next subsection. The average energy allocation policy implies that the transmit power at the relay is independent of the instantaneous channel fading and only depends on the amount of long-term harvested energy in one time slot. Thus, the transmit power of the relay remains same in any time slot as $P_k(t) = \kappa\eta P_s\Omega_{Sk}$, and the instantaneous SNRs of the links $\mathcal{S}\mathcal{R}_k$ and $\mathcal{R}_k\mathcal{D}$ in (4) and (6) is rewritten as

$$\gamma'_{Sk}(t) = \frac{P_s|h_{Sk}(t)|^2}{\sigma^2+\kappa\eta P_s\Omega_{Sk'}|h_{kk'}(t)|^2}, \tag{17}$$

$$\gamma'_{kD}(t) = \frac{\kappa\eta P_s\Omega_{Sk}|h_{kD}(t)|^2}{\sigma^2}. \tag{18}$$

Since all involved links follow independent Rayleigh fading, the corresponding CDFs of the above SNRS are given by

$$F_{\gamma_{Sk}}{}'(\gamma) = 1 - \frac{\exp\left(-\left(\sigma^2/\Omega_{Sk}P_s\right)\gamma\right)}{1+\kappa\eta\Omega_{Sk'}\Omega_{kk'}\gamma/\Omega_{Sk}}, \tag{19}$$

$$F_{\gamma_{kD}}{}'(\gamma) = 1 - \exp\left(-\frac{\sigma^2}{\kappa\eta P_s\Omega_{Sk}\Omega_{kD}}\gamma\right). \tag{20}$$

Then, the CDFs of the E2E SNRs as (11) and (12) are

$$F_{\gamma_{SkD}}{}'(\gamma) = 1 - \left[1-F_{\gamma_{Sk}}{}'(\gamma)\right]\left[1-F'_{\gamma_{kD}}(\gamma)\right]. \tag{21}$$

One may wonder that the consumed energy at the relay is constrained by the instantaneous status of energy storage.

This issue can be addressed by the energy reservation policy [56]. Assuming one transmission round consists of N time slots, at the beginning of each round, the energy storage has enough energy to support the whole round transmission due to the initial energy charging and the previous harvested energy, i.e., $E_r(0) \geq N(1-\alpha)TP_k/2$, so the energy depletion will never happen in this round. If N is large, the total harvested energy in this round is equal to the consumed energy. At the end of each round, the energy storage will be resupplied to the same energy level for next round operation. With the energy reservation policy, the instantaneous limitation of energy storage can be relaxed, and only the sustainable constraint needs to be guaranteed such that the average consumed energy per slot is always less than that of the harvested energy. Thus, the achievable throughput can be obtained in the following lemma.

Lemma 4. *If the relays are deployed with energy storages, the harvest-store-use energy management strategy can be utilized. Under average energy allocation, the achievable network throughput of the WPSR scheme is*

$$\begin{aligned}\tau_E &= \frac{1-\alpha}{2}\left\{\mathbb{E}\left[\log_2\left(1+\min\left\{\gamma'_{S1}(t),\gamma'_{1D}(t)\right\}\right)\right]\right. \\ &\quad \left.+\mathbb{E}\left[\log_2\left(1+\min\left\{\gamma'_{S2}(t-1),\gamma'_{2D}(t)\right\}\right)\right]\right\} \\ &= \frac{1-\alpha}{2}\sum_{k=1,2}\int_0^{+\infty}\log_2(1+\gamma){f_{\gamma_{SkD}}}'(\gamma)d\gamma.\end{aligned} \tag{22}$$

where ${f_{\gamma_{SkD}}}'(\gamma)$ *is presented in (21).*

4.1.4. WPSR with Both Data Buffers and Energy Storages. Lastly, we consider the case that the relays have both data buffers and energy storages. Based on the previous analysis, the achievable throughput can be presented in the following theorem.

Lemma 5. *If both data buffers and energy storages are exploited, the buffer-and-forward data management and harvest-store-use energy management strategies can be utilized. Thus, the corresponding achievable throughput of WPSR scheme is given by*

$$\begin{aligned}\tau_{B,E} &= \frac{1-\alpha}{2}\sum_{k=1,2}\min\left\{\mathbb{E}\left[\log_2\left(1+\gamma'_{Sk}(t)\right)\right],\mathbb{E}\left[\log_2\left(1+\gamma'_{kD}(t)\right)\right]\right\} \\ &= \frac{1-\alpha}{2}\sum_{k=1,2}\min\left\{\int_0^{+\infty}\log_2(1+\gamma){f_{\gamma_{Sk}}}'(\gamma)d\gamma,\int_0^{+\infty}\log_2(1+\gamma)f'_{\gamma_{kD}}(\gamma)d\gamma\right\}.\end{aligned} \tag{23}$$

Table 1 summarizes the achievable throughput of the WPSR scheduling schemes with and without data buffers and energy storages. Since $\mathbb{E}[\min\{x,y\}] \leq \min\{\mathbb{E}[x],\mathbb{E}[y]\}$, the data buffer always introduces throughput gain. If the relay is provisioned with energy storage and the average energy allocation policy is utilized, the transmit power at the relay only depends on the statistical channel state and becomes $2\alpha/(1-\alpha)\eta P_s\Omega_{Sk}$ instead of $2\alpha/(1-\alpha)\eta P_s|h_{Sk}(t)|^2$. Furthermore, the effect of energy storage is analyzed in the following corollary.

Corollary 6. *If the relay is deployed with energy storage and average energy allocation policy is utilized, the achieved rate of the link from the source to the relay is degraded due to the inter-relay-interference (IRI), while that of the link from the relay to destination, which is usually the weak and bottleneck channel, is improved.*

As $\log_2(1+a/x)$ and $\log_2(1+bx)$ are convex and concave functions, respectively, we have $\mathbb{E}[\log_2(1+a/x)] \geq \log_2(1+a/\mathbb{E}[x])$ and $\mathbb{E}[\log_2(1+bx)] \leq \log_2(1+b\mathbb{E}[x])$ by Jensen inequality. Thus, the Corollary 6 can be concluded.

Above all, data buffers at the relays can always bring throughput gain, and with energy storages, the energy allocation policy can be applied to efficiently use the harvested energy to improve the achieved network throughput.

4.2. Adaptive Wireless Powered Buffer-Aided Successive Relaying (WPBSR) Scheme. To further improve the achievable network throughput, in this subsection, adaptive resource management (i.e., time and energy allocation) is incorporated to explore the potential of data buffers and energy storages at the relays.

In general, both hops from the source to the relays and from the relays to the destination usually experience the different channel conditions, and there exists a gap between the achievable rates of both hops. Thus, instead of the time scheduling manner in the previous section, it is necessary to efficiently allocate the transmission time according to the dynamic system states, namely, adaptive time allocation, to maximize the network throughput. Hence, as presented in Section 3, one time slot is splitted into three subslots, in which each subslot is associated with one transmission mode, i.e., WET, WIT-I with $\mathscr{R}_1$ reception, and WIT-II with $\mathscr{R}_2$ reception. Define $m_l(t) \in [0,1]$, $(l \in \{1,2,3\})$ as the time ratio allocated to the l-th transmission mode in the t-th time slot. Thus, the time ratio vector $m(t) = (m_1(t), m_2(t), m_3(t))$ satisfies

$$\sum_l m_l(t) \leq 1, m_l(t)[m_l(t)-1] \leq 0, \forall l \in \{1,2,3\}. \tag{24}$$

In WET, the source charges both relays by exploring RF energy harvesting technology. We define $e_k^h(t)$ as the amount of harvested energy at the relay $\mathscr{R}_k$ in time slot t, which is given by

$$0 \leq e_k^h(t) \leq m_1(t)T\eta P_s|h_{Sk}(t)|^2. \tag{25}$$

In WIT-I mode, $\mathscr{R}_1$ receives information from the source, and $\mathscr{R}_2$ forwards buffered data to the destination. Thus, there exists the inter-relay-interference (IRI) between both relays, and the signals received at $\mathscr{R}_1$ and $\mathscr{D}$ are given in (3) and (5), respectively. Denote $R_{S1}(t), R_{2D}(t)$ as the

Table 1: Throughput comparison of WPSR schemes with and without data buffer and energy storage.

Network Scenarios	Achievable Network Throughput
Without Data Buffers and Energy Storages	$\sum_k \frac{1-\alpha}{2}\mathbb{E}\left[\min\left\{\log_2\left(1+\frac{P_s\lvert h_{Sk}(t)\rvert^2}{\sigma_k^2+(2\alpha/1-\alpha)\eta P_s\lvert h_{Sk'}(t)\rvert^2}\right),\log_2\left(1+\frac{(2\alpha/1-\alpha)\eta P_s\lvert h_{Sk}(t)\rvert^2\lvert h_{kD}(t)\rvert^2}{\sigma_d^2}\right)\right\}\right]$
With Only Data Buffers	$\sum_k \frac{1-\alpha}{2}\min\left\{\mathbb{E}\left[\log_2\left(1+\frac{P_s\lvert h_{Sk}(t)\rvert^2}{\sigma_k^2+(2\alpha/1-\alpha)\eta P_s\lvert h_{Sk'}(t)\rvert^2\lvert h_{kk'}(t)\rvert^2}\right)\right],\mathbb{E}\left[\log_2\left(1+\frac{(2\alpha/1-\alpha)\eta P_s\lvert h_{Sk}(t)\rvert^2\lvert h_{kD}(t)\rvert^2}{\sigma_d^2}\right)\right]\right\}$
With Only Energy Storages	$\sum_k \frac{1-\alpha}{2}\mathbb{E}\left[\min\left\{\log_2\left(1+\frac{P_s\lvert h_{Sk}(t)\rvert^2}{\sigma_k^2+(2\alpha/1-\alpha)\eta P_s\Omega_{sk'}\lvert h_{kk'}(t)\rvert^2}\right),\log_2\left(1+\frac{(2\alpha/1-\alpha)\eta P_s\Omega_{sk}\lvert h_{kD}(t)\rvert^2}{\sigma_d^2}\right)\right\}\right]$
With Data Buffers and Energy Storages	$\sum_k \frac{1-\alpha}{2}\min\left\{\mathbb{E}\left[\log_2\left(1+\frac{P_s\lvert h_{Sk}(t)\rvert^2}{\sigma_k^2+(2\alpha/1-\alpha)\eta P_s\Omega_{Sk'}\lvert h_{kk'}(t)\rvert^2}\right)\right],\mathbb{E}\left[\log_2\left(1+\frac{(2\alpha/1-\alpha)\eta P_s\Omega_{Sk}\lvert h_{kD}(t)\rvert^2}{\sigma_d^2}\right)\right]\right\}$

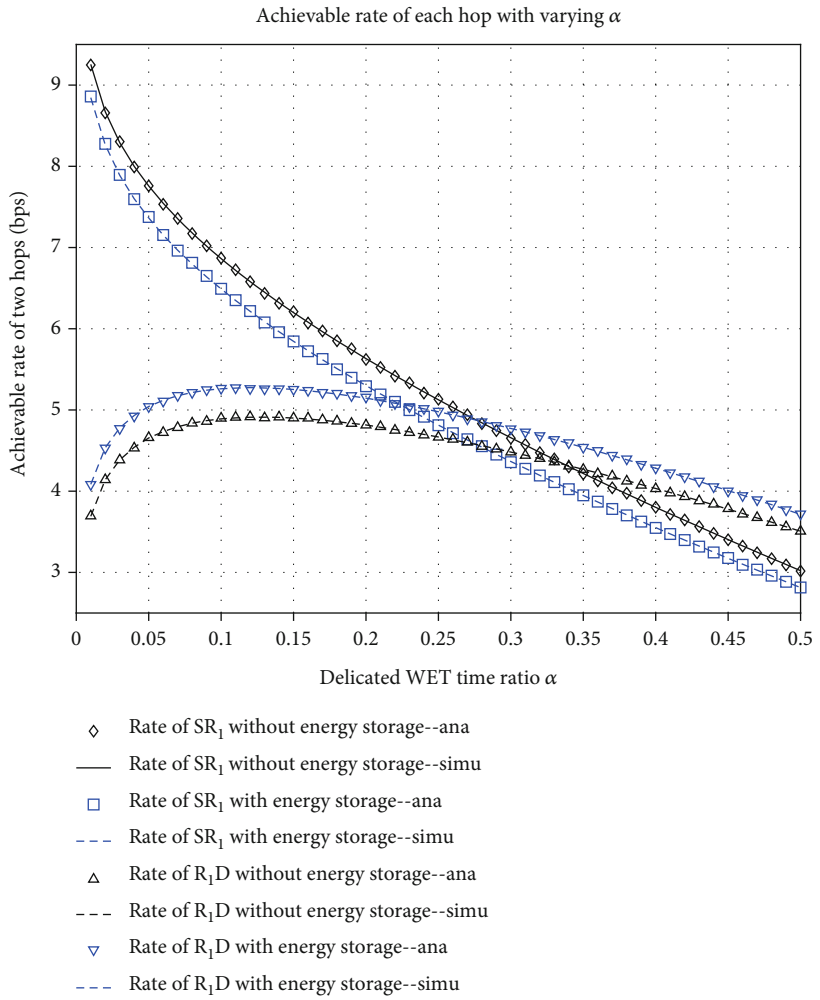

Figure 3: Achievable throughput of each hop with and without energy storages at the relays.

amount of transmitted information bits on the links $\mathcal{S}\mathcal{R}_1$ and $\mathcal{R}_2\mathcal{D}$, respectively, and they satisfy

$$0 \le R_{S1}(t) \le m_2(t)\, T \log_2\left(1 + \frac{P_s|h_{S1}(t)|^2}{\sigma^2 + P_2(t)|h_{12}(t)|^2}\right), \quad (26)$$

$$0 \le R_{2D}(t) \le m_2(t) T \log_2\left(1 + \frac{P_2(t)|h_{2D}(t)|^2}{\sigma^2}\right). \quad (27)$$

Similarly, in WIT-II mode, the amount of transmitted bits on the links $\mathcal{S}\mathcal{R}_2$ and $\mathcal{R}_1\mathcal{D}$ are defined as $R_{S2}(t)$, $R_{1D}(t)$, which are given by

$$0 \le R_{S2}(t) \le m_3(t) T \log_2\left(1 + \frac{P_s|h_{S2}(t)|^2}{\sigma^2 + P_1(t)|h_{12}(t)|^2}\right), \quad (28)$$

$$0 \le R_{1D}(t) \le m_3(t) T \log_2\left(1 + \frac{P_1(t)|h_{1D}(t)|^2}{\sigma^2}\right). \quad (29)$$

Meanwhile, the consumed energy $e_1^c(t), e_2^c(t)$ at both relays are

$$e_1^c(t) = m_3(t) P_1(t) T, \quad (30)$$

$$e_2^c(t) = m_2(t) P_2(t) T. \quad (31)$$

To achieve the maximum throughput, the long-term buffer stability constraint (namely, the average arrival rate of data buffer is same with the allowed departure rate) needs to be satisfied, i.e.,

$$\frac{1}{N}\sum_{t=1}^{N} R_{Sk}(t) = \frac{1}{N}\sum_{t=1}^{N} R_{kD}(t), \forall k \in \{1, 2\}. \quad (32)$$

Similarly, to realize perpetual operation, the energy sustainable constraint is that the average amount of the

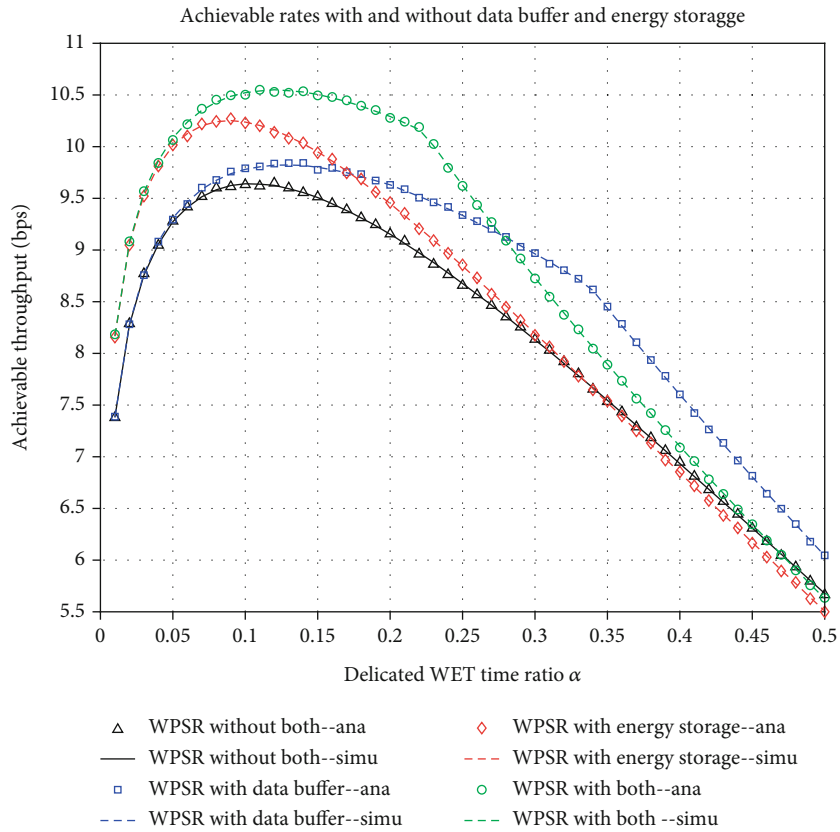

Figure 4: Achievable throughput of WPSR schemes with and without data buffers and energy storages.

consumed energy is not larger than that of the harvested energy, i.e.,

$$\frac{1}{N}\sum_{t=1}^{N} e_k^c(t) \le \frac{1}{N}\sum_{t=1}^{N} e_k^h(t), \forall k \in \{1,2\}. \tag{33}$$

Thus, we formulate the following optimization problem that maximizes the network throughput under the constraints of the buffer stability and the energy sustainability, i.e.,

$$\begin{aligned} \max_{m(t),P(t)} \quad & \frac{1}{N}\sum_{t=1}^{N} [R_{S1}(t) + R_{S2}(t)] \\ \text{s.t.} \quad & (24) - (24)(33), \end{aligned} \tag{34}$$

where both the transmit powers at the relays $P(t) = (P_1(t), P_2(t))$ and the time scheduling $m(t) = (m_1(t), m_2(t), m_3(t))$ are jointly optimized. The constraints (32) and (33) specify the long-term average constraints and the others indicate the constraints that must be satisfied in each time slot. Noting that for the system with either data buffer or energy storage, the corresponding resource allocation problem can be derived by slacking and rewriting part of the constraints. Due to the nonconvex constraints (26) and (28), the problem (34) is nonconvex and difficult to be directly solved. Instead, we explore the Lyapunov optimization [55] to address it and obtain the adaptive resource allocation scheme. By applying such method, the instantaneous status of data buffer and energy storage is utilized as well. Thus, the precaching procedure [53] to guarantee the nonempty data buffer, and the energy reservation policy to prevent energy depletion, is no longer necessary.

Define $Q(t) = (Q_1(t), Q_2(t))$ and $E(t) = (E_1(t), E_2(t))$ as the status of data buffers and energy storages in time slot t, respectively, which are updated as

$$Q_k(t+1) = \max[Q_k(t) - R_{kD}(t), 0] + R_{Sk}(t), \tag{35}$$

$$E_k(t+1) = E_k(t) - e_k^c(t) + e_k^h(t). \tag{36}$$

Similar to Theorem 2.5 in [57], the long-term average constraints in (32) and (33) can be converted into the queues stability constraints. For the constraint (33), we can construct a virtual energy queue, in which the consumed energy $e_k^c(t)$ and the harvested energy $e_k^h(t)$ correspond to the arrival and departure process, respectively. Comparing with (36), we can observe that the constructed energy queue is opposite to the energy storage. Thus, we may denote $\phi_k - E_k(t)$ as the constructed energy queue and its evolution expression is

$$\phi_k - E_k(t+1) = \phi_k - E_k(t) - e_k^h(t) + e_k^c(t). \tag{37}$$

Here, the energy queue $\phi_k - E_k(t)$ can be interpreted as virtual vacant energy storage. In Lemma 9 of Subsection 4.3, we will show that ϕ_k can be considered as a bound of virtual energy storage. Then, we have the generalized queue $\Theta(t) = [Q(t); \phi - E(t)]$, where $\phi = (\phi_1, \phi_2)$, and define the following Lyapunov function and one-slot conditional Lyapunov drift as

$$L(\Theta(t)) = \frac{1}{2}\sum_k \lambda_k Q_k(t)^2 + \frac{1}{2}\sum_k \mu_k[\phi_k - E_k(t)]^2, \quad (38)$$

$$\Delta(\Theta(t)) = \mathbb{E}[L(\Theta(t+1)) - L(\Theta(t))|\Theta(t)], \quad (39)$$

where λ_k, μ_k are nonnegative parameters to quantify the relative effect of data buffer and energy queue, and the Lyapunov drift characterizes the increment of the generalized queue.

To maximize the achievable throughput with queue stable constraints, we aim to not only minimize the increment of generalized queue but also maximize the transmission rate. Thus, we need to minimize the drift-plus-penalty function $\Delta(\Theta(t)) - V\sum_k \mathbb{E}[R_{Sk}(t)|\Theta(t)]$, where V is a nonnegative control parameter to quantify the tradeoff of queue backlog and the average achievable throughput. The following proposition provides us an upper bound of the drift-plus-penalty function.

Proposition 7. *Given the i.i.d. channel gain, the drift-plus-penalty is bounded by*

$$\begin{aligned}\Delta(\Theta(t)) - V\sum_{k\in\{1,2\}} \mathbb{E}[R_{Sk}(t)|\Theta(t)] \le B - \sum_{k\in\{1,2\}} \\ \Big\{V\mathbb{E}[R_{Sk}(t)|\Theta(t)] + \lambda_k Q_k(t)\mathbb{E}[R_{Sk}(t) - R_{kD}(t)|\Theta(t)] \\ + \mu_k[\phi_k - E_k(t)]\mathbb{E}\left[e_k^c(t) - e_k^h(t)\middle|\Theta(t)\right]\Big\},\end{aligned} \quad (40)$$

where B is a finite constant and can be given as

$$\begin{aligned}B \ge \sum_{k\in\{1,2\}} \Bigg\{\frac{\lambda_k}{2}\mathbb{E}\left[\left((R_{Sk}(t))^2 + (R_{kD}(t))^2\right|\Theta(t)\right] \\ + \frac{\mu_k}{2}\mathbb{E}\left[\left(e_k^c(t) - e_k^h(t))^2|\Theta(t)\right)\right]\Bigg\}.\end{aligned} \quad (41)$$

The procedure of how to derive the above upper bound is similar to Lemma 4.6 in [55]. With Proposition 7, instead of directly minimizing the drift-plus-penalty item, the scheduling scheme actually seeks to minimize its upper bound in (40). Thus, we propose an adaptive wireless powered buffer-aided successive relaying (WPBSR) scheme, which performs the following operations in each time slot according to the current channel state $h(t)$ and queue status $\Theta(t)$.

(i) *Joint Time Allocation and Power Allocation*. Determining $m(t), P(t)$ by solving the following optimization problem:

$$\begin{aligned}\min_{\mathrm{m(t),P(t)}} \quad \sum_{k\in\{1,2\}} [\lambda_k Q_k(t) - V]R_{Sk}(t) - \lambda_k Q_k(t)R_{kD}(t) \\ + \mu_k[\phi_k - E_k(t)]\left[e_k^c(t) - e_k^h(t)\right] \\ \text{s.t.}(24) - (24)(31).\end{aligned} \quad (42)$$

(ii) *Update Queue State*. Update all queues state as (35) and (37), respectively

The problem (42) seeks to jointly maximize the weighted transmission rate and minimize the weighted consumed energy, where the weighting value relies on the status of the corresponding data buffers and energy storages. In fact, only the constraints (26), (27), and (31) are associated with $P_2(t)$, and (28), (29), and (30) are dependent on $P_1(t)$. Thus, the optimization decomposition technology can be used. We firstly minimize the associated terms with respect to $P_1(t)$ and $P_2(t)$ under given $m_3(t)$ and $m_2(t)$, respectively, to derive the power allocation scheme. Then, we minimize the objective with respect to $m(t)$ by inserting the optimal $P_1(t), P_2(t)$ into (42) to obtain the time allocation scheme.

In WET mode, the problem is to determine the amount of charged energy into the energy storage of each relay, i.e.,

$$L_1^* = \min_{e_1^h(t), e_2^h(t)} \; -\sum_{k\in 1,2} \mu_k[\phi_k - E_k(t)]e_k^h(t) \text{s.t.} \quad (25), \quad (43)$$

where the scheduling reward $-L_1^*$ is the weighted sum of the charged energy at both relays. If $E_k(t) < \phi_k$, we have $e_k^h(t) = m_1(t)T\eta P_s|h_{S1}(t)|^2$ and otherwise $e_k^h(t) = 0$. This implies that, when the stored energy is not enough, the energy harvesting unit will convert all energy of the received signal to charge the energy storage, otherwise, it will not work.

In WIT-I mode with $\mathscr{R}_1$ reception, the power allocation problem is to determine the power $P_2(t)$ with given $m_2(t)$, which can be rewritten as

$$\begin{aligned}L_2^* = \min_{P_2(t)\in\left[0, \frac{E_2(t)}{T}\right]} \; -[V - \lambda_1 Q_1(t)]R_{S1}(t) - \lambda_2 Q_2(t)R_{2D}(t) \\ + \mu_2[\phi_2 E_2(t)]e_2^c(t) \text{ s.t.}(26), (26)(27), (26)(27)(31),\end{aligned} \quad (44)$$

where the scheduling reward $-L_2^*$ equals the sum of weighted rate in the link $\mathscr{S}\mathscr{R}_1$ and $\mathscr{R}_2\mathscr{D}$ plus the weighted consumed energy. Noting that different links have different weighting coefficients, i.e., the weighting coefficient of the link $\mathscr{S}\mathscr{R}_1$ is $V - \lambda_1 Q_1(t)$, and the weighting coefficient of the link $\mathscr{R}_2\mathscr{S}$ is $\lambda_2 Q_2(t)$. This means that larger data buffer length always indicates larger weighting coefficient of the

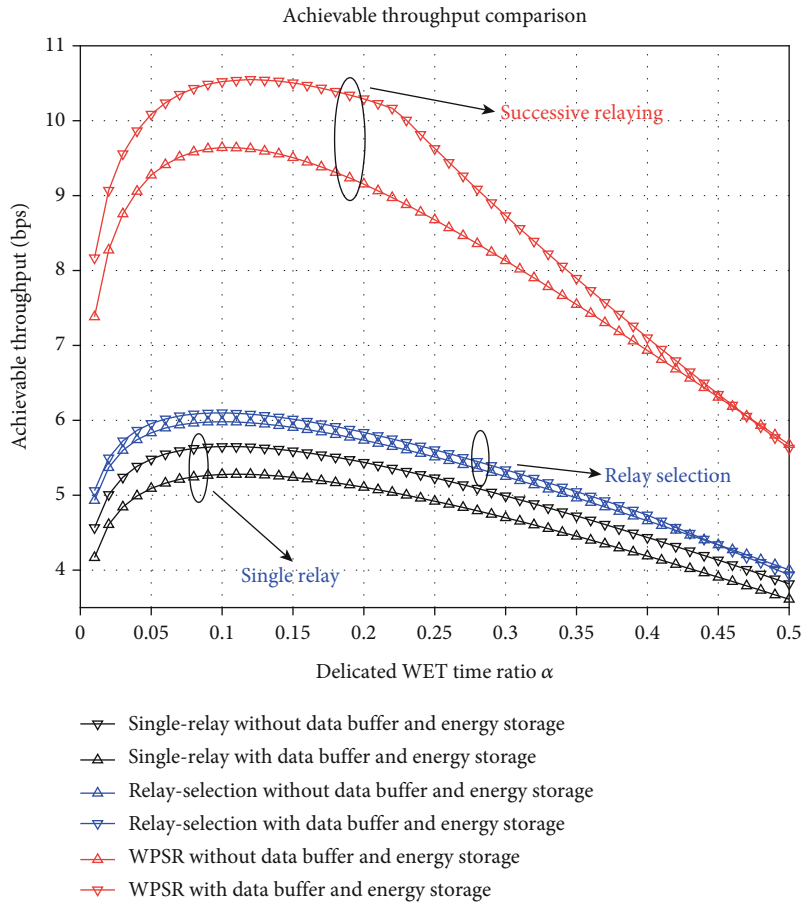

Figure 5: Achievable throughput comparison of one and two relays networks.

links from the relay to the destination and the smaller weighting coefficient of the links from the source to the relay in order to decrease the length of data buffer and keep it stable. There are two cases concerning the relationship between V and $\lambda_1 Q_1(t)$.

(1) $\lambda_1 Q_1(t) \geq V$. In this case, we have $R_{S1}(t) = 0$, which means no information transmission on the link $\mathcal{S}$ $\mathcal{R}_1$ as large data buffer length at the relay $\mathcal{R}_1$. Therefore, this case will be degenerated into the single-relay selection policy instead of successive relaying. By taking derivation with respect to $P_2(t)$, the power $P_2(t)$ at the relay $\mathcal{R}_2$ can be obtained as

$$P_2(t) = \left[\frac{\lambda_2 Q_2(t)}{\ln 2\mu_2[\phi_2 - E_2(t)]} - \frac{\sigma^2}{|h_{2D}(t)|^2}\right]^{\dagger}, \quad (45)$$

where $[x]^{\dagger} = \max\{\min\{x, E_2(t)/T\}, 0\}$. The power allocation strategy is similar to the water-filling mode, and it also relies on the data buffer status $Q_2(t)$ and energy storage status $E_2(t)$. Either a larger data buffer status or a larger energy storage status leads to a larger transmit power at the relay $\mathcal{R}_2$.

(2) $\lambda_1 Q_1(t) < V$. In this case, we have $R_{S1}(t) = m_2(t)T \log_2(1 + P_s|h_{S1}(t)|^2/\sigma^2 + P_2(t)|h_{12}(t)|^2)$, and the corresponding power allocation problem can be rewritten as

$$\begin{aligned}\min_{P_2(t)\in\left[0,\frac{E_2(t)}{T}\right]} \quad & [\lambda_1 Q_1(t) - V]\log_2\left(1 + \frac{P_s|h_{S1}(t)|^2}{\sigma^2 + P_2(t)|h_{12}(t)|^2}\right) \\ & - \lambda_2 Q_2(t)\log_2\left(1 + \frac{P_2(t)|h_{2D}(t)|^2}{\sigma^2}\right) \\ & + \mu_2[\phi_2 - E_2(t)]P_2(t).\end{aligned} \quad (46)$$

Since $\log_2(1 + P_s|h_{S1}(t)|^2/(\sigma^2 + P_2(t)|h_{12}(t)|^2))$ and $\log_2(1 + P_2(t)|h_{2D}(t)|^2/\sigma^2)$ are convex and concave function with respect to $P_2(t)$, respectively, the problem becomes concave-convex procedure (CCP) [58]. On one hand, the convex-concave optimization algorithm [59] can be utilized. On the other hand, as $P_2(t)$ is the only optimization variable, we can find out that the molecular term of the $P_2(t)$ is a cubic function [60], and there are many existing methods

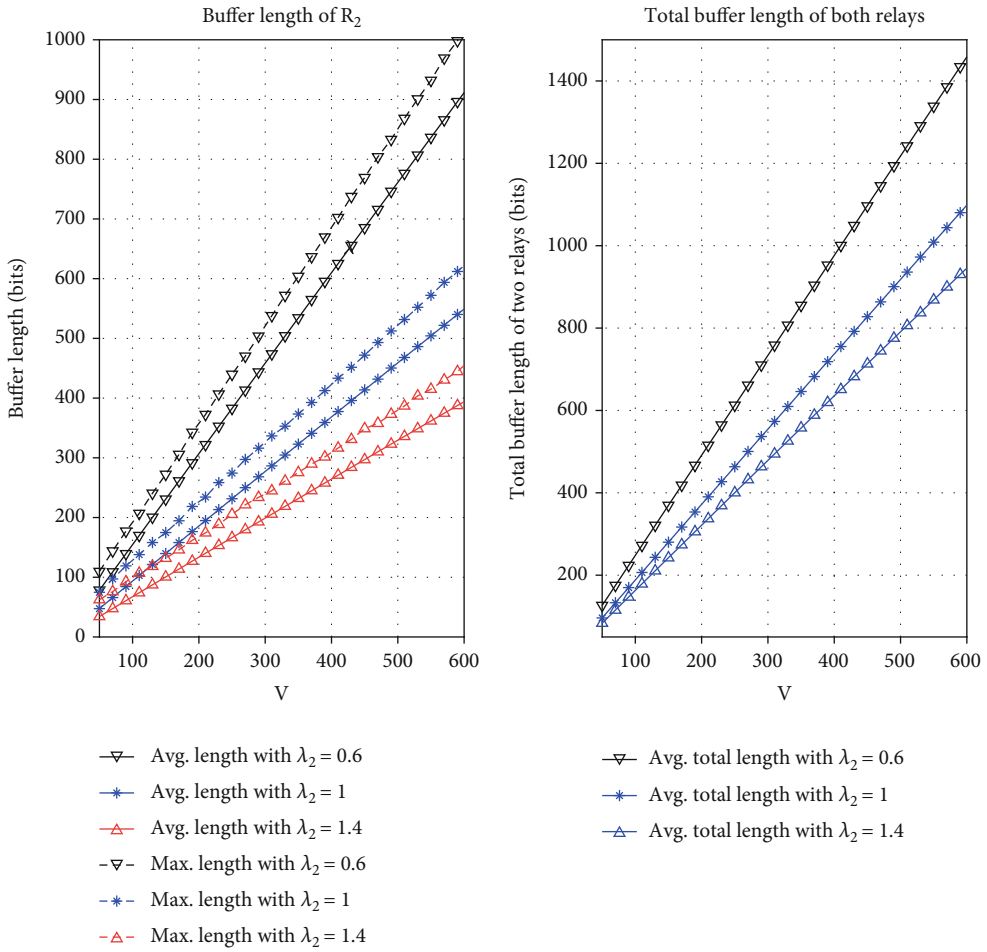

Figure 6: Average and maximal buffer lengths of the relays with varying V.

to derive the stationary points, namely, the optimal transmit power $P_2^*(t)$.

In WIT-II mode with $\mathscr{R}_2$ reception, the corresponding power allocation problem can be rewritten as

$$L_3^* = \min_{P_1(t)\in\left[0,\frac{E_1(t)}{\tau}\right]} [\lambda_2 Q_2(t) - V]R_{S2}(t) - \lambda_1 Q_1(t)R_{1D}(t) + \mu_1[\phi_1 - E_1(t)]e_1^c(t) \text{s.t.} (28), (28)(29), (28)(29)(30). \tag{47}$$

Likewise, we can derive the optimal power allocation $P_1^*(t)$ as (44).

Then, the second step is to optimize the time allocation $m(t)$ with the given allocated power $P^*(t)$. The problems (44) and (47) indicate that the optimally allocated power $P_1^*(t), P_2^*(t)$ are independent of $m(t)$, and the time allocation problem is a standard linear problem, thus, the optimal $m_k^*(t)$ is either zero or one. Such that we can summarize the adaptive wireless powered buffer-aided successive relaying (WPBSR) scheme in the following theorem.

Theorem 8. *The adaptive wireless powered buffer-aided successive relaying (WPBSR) scheme is to allocate the time slot to the transmission mode with the largest scheduling reward, i.e.,*

$$l^* = argmax - L_l^* \tag{48}$$

where the scheduling rewards $-L_1^*, -L_2^*, -L_3^*$ are obtained by solving (43), (44), and (47), l^* represents the selected "best" mode.

4.3. Performance Analysis. In this subsection, we will analyze the achieved performance of the proposed WPBSR scheme. We firstly investigate the upper bound of instantaneous data buffer and energy storage length in the following lemma, which validates that the finite data buffer and energy storage are guaranteed.

Lemma 9. *If the channel coefficients of the links $\mathscr{SR}_k$ are bounded, i.e., $\tilde{h}_{Sk}(t) \le \tilde{h}_{Sk}^{\max}$, the lengths of data buffer and energy storage are also bounded as*

$$Q_k(t) < \frac{V}{\lambda_k} + R_{Sk}^{\max}, E_k(t) \le \phi_k + e_k^{\max}, \forall t, \forall k, \tag{49}$$

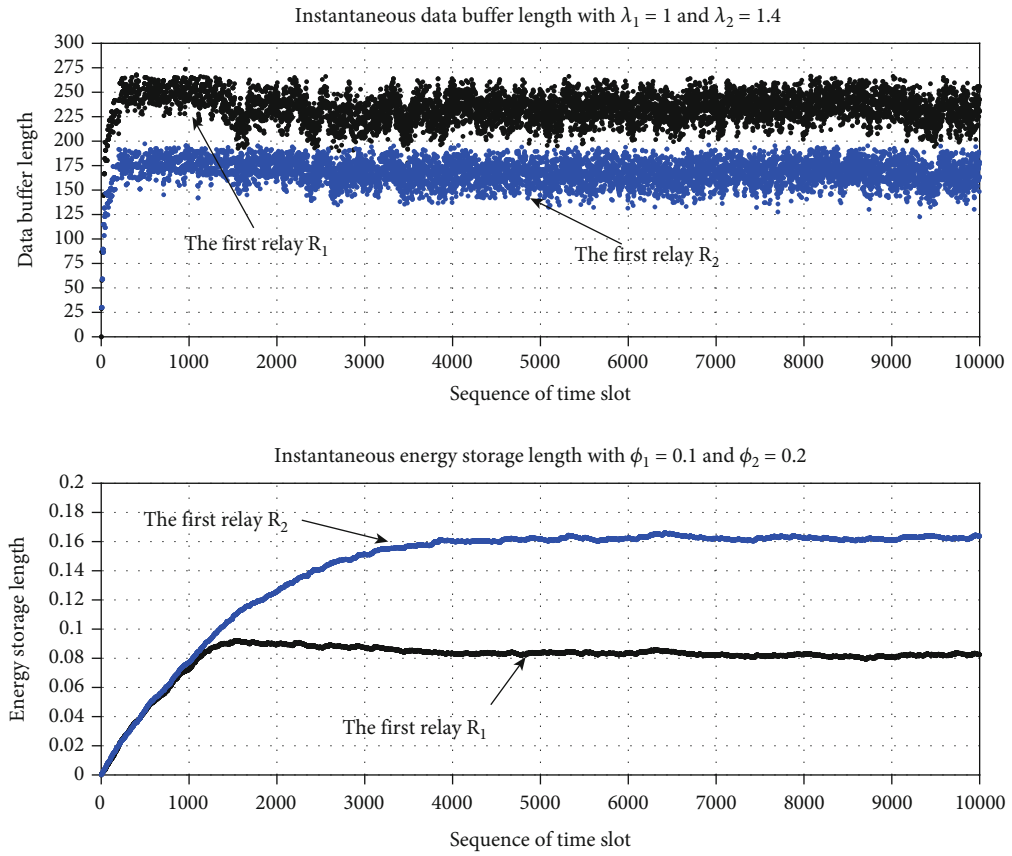

FIGURE 7: Instantaneous data buffer and energy storage length with $V = 250$.

where $R_{Sk}^{\max} = T\log_2(1 + P_s L_{Sk}\tilde{h}_{Sk}^{\max}/\sigma^2)$ *and* $e_k^{\max} = T\eta P_s L_{Sk}\tilde{h}_{Sk}^{\max}$ *are the maximal transmission rate from the source to the relay and the maximal amount of harvested energy at the relay in one time slot, respectively.*

Proof. Given (35), we have $Q_k(t+1) \le Q_k(t) + R_{Sk}(t)$. In the adaptive WPBSR scheduling scheme, $\lambda_k Q_k(t) \ge V$ yields $R_{Sk}(t) = 0$, which means the data buffer length will not increase when it is larger than V/λ_k. Thus, the instantaneous data buffer length satisfies $Q_k(t+1) < V/\lambda_k + R_{Sk}(t)$. As the bounded channel gain results $R_{Sk}(t) \le R_{Sk}^{\max}$, the upper-bound of data buffer is derived. Similar procedure is applied for the energy storage. □

According to Lemma 9, the bound of the data buffer $Q_k(t)$ is linearly and inversely propositional to V and λ_k, respectively. Meanwhile, the bound of the energy storage $E_k(t)$ is linearly propositional to ϕ_k. This implies our proposed WPBSR scheme is also effective for the case that two relays have different limits of the data buffers and energy storages. Given the limits of the data buffer and energy storage, the parameters λ_k, ϕ_k can be determined as well. Noting that there exists similar characteristics under unbounded channel gain, in which the instantaneous data buffer length still satisfies $Q_k(t+1) < V/\lambda_k + R_{Sk}(t)$. However, unbounded channel gain can only guarantee that $R_{Sk}(t)$ is less than a finite value with large probability instead of a limit.

Second, we study the queue stability and average achievable performance of the proposed scheme, including average data buffer length, network throughput, and average transmission delay.

Theorem 10. *For any parameter $V > 0$, there exist the constants of $B \ge 0, \varepsilon \ge 0, \Psi(\varepsilon)$, where $\Psi(\varepsilon)$ is less than the optimal throughput R^{opt}, such that the adaptive WPBSR scheme will exhibit the following properties:*

(1) All data buffer queue $Q_k(t)$ and energy queue $\phi_k - E_k(t)$ are mean rate stable, thus, the constraints (32) and (33) in problem (34) are guaranteed

(2) The achievable throughput and the average buffer length are bounded as below

$$R^{opt} - \frac{B}{V} \le \lim_{N\longrightarrow\infty} \frac{1}{N}\sum_{t=0}^{N-1} \mathbb{E}[R_{S1}(t) + R_{S2}(t)] \le R^{opt}, \tag{50}$$

$$\lim_{N\longrightarrow\infty} \frac{1}{N}\sum_{t=0}^{N-1} \sum_{k\in\{1,2\}} \mathbb{E}[\lambda_k Q_k(t)] \le \frac{B + \left[R^{opt} - \Psi(\varepsilon)\right]V}{\varepsilon}. \tag{51}$$

Proof. Please see Appendix 9.

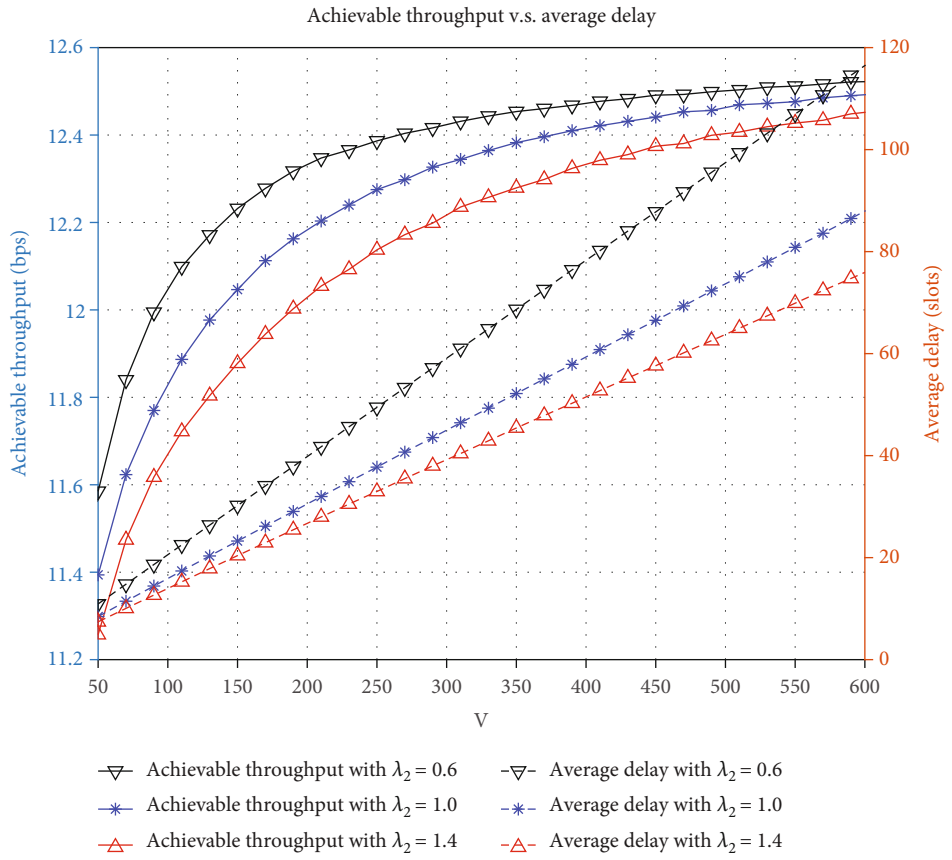

FIGURE 8: Achievable throughput and average delay of the adaptive WPBSR scheme with varying V.

According to (48), we know that the average buffer length of the relay $\mathscr{R}_k$ is bounded by $B + [R^{\text{opt}} - \Psi(\varepsilon)]V/\varepsilon\lambda_k$, which means a larger λ_k results in a smaller buffer length. Meanwhile, we can observe that the bound of the average data buffer length is proportional to V, while the time average achievable throughput can be arbitrarily close to the optimal network throughput as V increases. This implies a trade-off of $[O(V), O(1/V)]$ between the buffer length and the performance gap to the optimal achievable throughput. The average delay is computed by using Little's theorem as below

$$\bar{D} = \frac{1/N\sum_{t=1}^{N-1}\sum_k \mathbb{E}[Q_k(t)]}{1/N\sum_{t=1}^{N-1}\sum_k \mathbb{E}[R_{Sk}(t)]} \leq \frac{BV + [R^{\text{opt}} - \Psi(\varepsilon)]V^2}{\varepsilon[R^{\text{opt}}V - B]\max\{\lambda_1, \lambda_2\}}. \tag{52}$$

If V is large enough, the average delay is approximated as $\bar{D} \leq B + [R^{\text{opt}} - \Psi(\varepsilon)]V/\varepsilon R^{\text{opt}} \max\{\lambda_1, \lambda_2\}$, namely, the average delay increase linearly with V. □

Lastly, the implementation issues are investigated. As illustrated in Theorem 8, the optimal time scheduling is to choose the transmission mode with the largest scheduling reward. Its computation complexity can be ignored. Meanwhile, the optimal power allocation at the relays can be derived by (44) and (47), and the computation complexity mainly depends on solving the cubic function. Therefore, the computation complexity is not a critical issue.

Similar with [22], the centralized scheduling manner is assumed, in which the destination node acts as the control node. Of course, the similar analysis can be readily generalized to the case when other node, for instance, the source node, is the central control node. The destination needs to collect CSIs, BSIs, and ESIs and then informs its decision to the other nodes. The whole procedure may work at the beginning of each time slot as follows: (a) the source transmits the pilot symbol, from which both relays acquire the CSIs of the source-to-relay channel; (b) the destination obtains the relays-to-destination CSI from the pilots transmitted by the relays; (c) the relays reports the source-to-relay CSI, its BSI and ESI to the destination; (d) when the destination collect all the above information, the optimal power and time allocation can be decided based on (43), (44), (47), and Theorem 8; (e) the destination broadcasts a control message to both relays, which contains the knowledge of the optimal transmission mode and power. If WET mode is selected, the first relay informs the source. Accordingly, we can assess the required communication overhead. Three pilot insertions are required for CSI acquisitions, two control messages are required for both relays to report the information to the destination, and another one or two control messages are needed by the destination to inform the relays or the source the scheduling decisions.

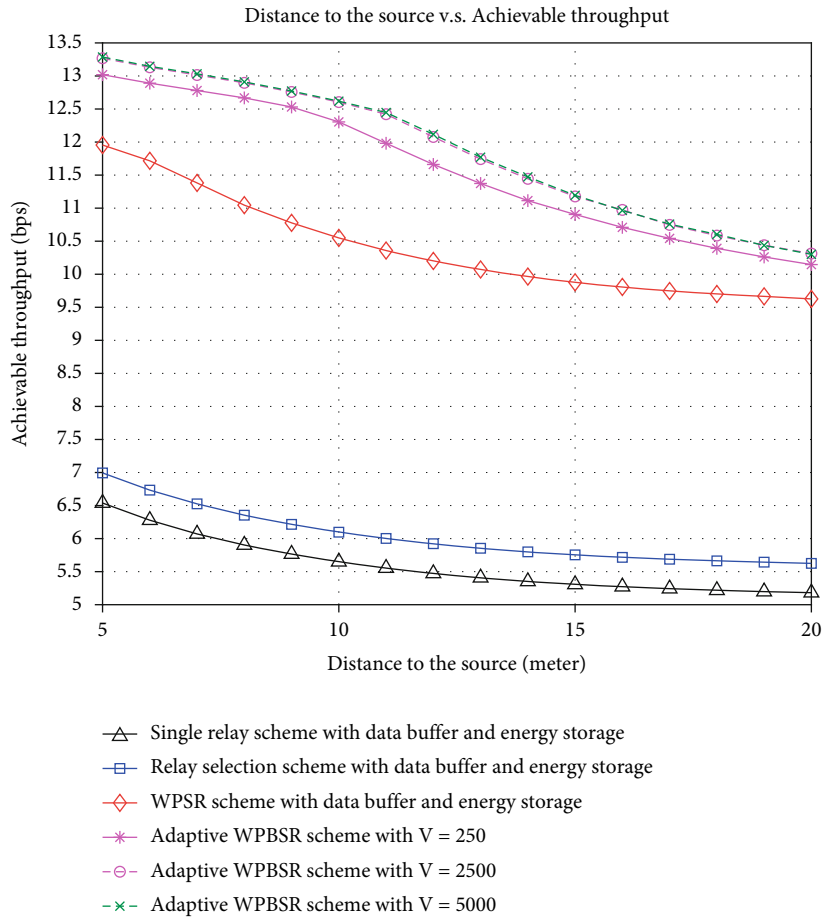

Figure 9: Achievable throughput with different distance between the source and the relays.

5. Performance Evaluation

In this section, we evaluate the performance of the proposed wireless powered successive relaying (WPSR) schemes. Unless otherwise stated, we consider the following network: the distance d_{SD} is 30 meters, the distances between the source and two relays are $d_{S1} = d_{S2} = 10$ meters, and the angle between the lines from the source to the relay and from the source to the destination is $\theta = \pi/8$. Therefore, the distance between two relays and the destination satisfy $d_{1D} = d_{2D} = \sqrt{d_{S1}^2 + d_{SD}^2 - 2d_{S1}d_{SD}\cos\theta}$, and the distance between both relays is $d_{12} = 2d_{S1}\sin\theta$. Meanwhile, we set the path loss exponent $m = 2.7$, the reference path loss $L_0 = 0.1$ at the reference distance $d_0 = 1$ meter, and the energy conversion efficiency is $\eta = 0.5$. The noise power is $\sigma^2 = -100$ dBm. The power of the source is $P_s = 30$ dBm.

5.1. Performance Comparison of WPSR with and without Data Buffers and Energy Storages. We first assess the performance of WPSR schemes in four network scenarios with and without data buffers and energy storages. When $\alpha \in [0.5,1]$, the achievable rates of both hops are decreasing as the insufficient WIT time, and the maximal throughput is achieved only in the region $\alpha \in [0,0.5]$. Therefore, we only present the results under $\alpha \in [0,0.5]$. Figure 3 presents the achievable throughput of the links between the source (or destination) and the relay with and without energy storage. When the energy storage is employed at the relay, the achievable rate of the link from the relay to the destination, which is usually the bottleneck link, is improved, while the rate of the link between the source and the relay degrades. This result is consistent with the Corollary 6, which unveils that the energy storage is able to balance the gap of both hops via the energy allocation, and improve the achievable throughput.

Figure 4 compares the achievable throughput of the WPSR schemes with and without data buffers and energy storages. As is shown, the simulation results are consistent with our analysis, and the WPSR schemes with data buffers always outperform that without data buffers. In the case of smaller α, i.e., $\alpha \in [0,0.3]$, the WPSR schemes with energy storages only can also bring throughput gain as well. However, with the further increase in α, especially when $\alpha > 0.34$, the WPSR schemes with energy storages only can not bring throughput gain, since now the channel from the source to the relay becomes the bottleneck link, which is consistent with the results in Figure 3. Above all, the data buffer can always improve the throughput performance, while the energy storage only may not always introduce

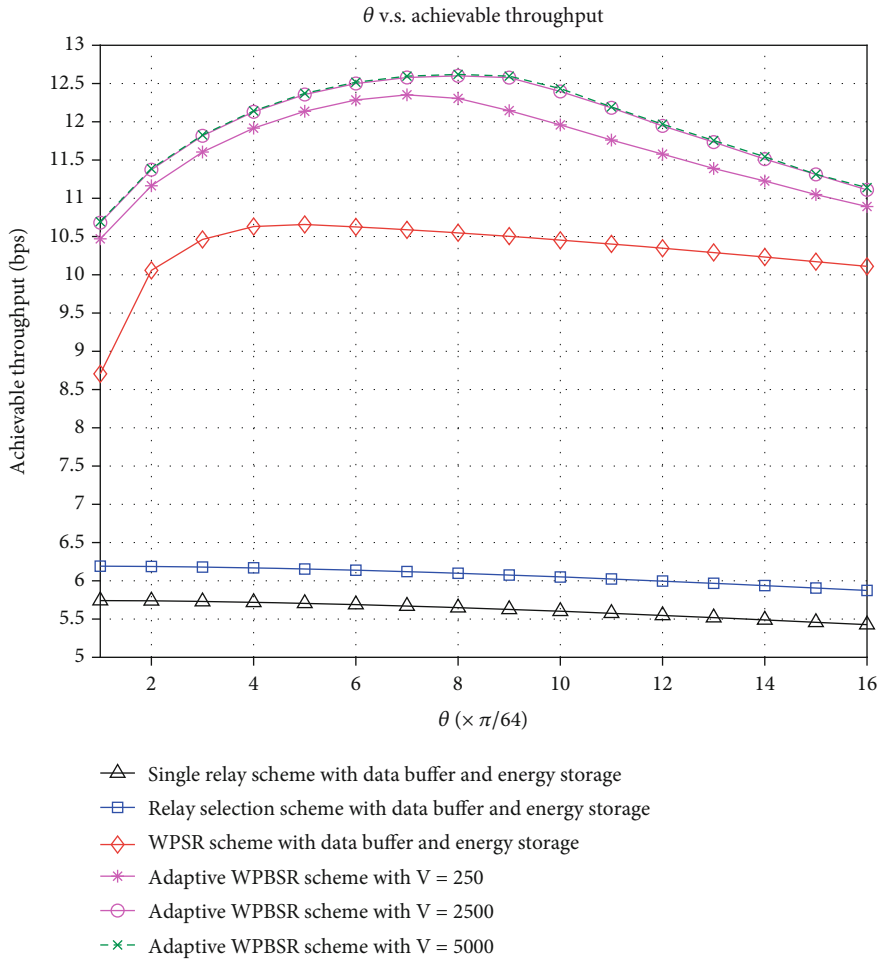

Figure 10: Achievable throughput with different angle θ.

throughput gain. While there exists a gap between the optimal achievable rate of the first hop and the rate of the second hop. Thus, the adaptive WPBSR scheduling scheme with both data buffers and energy storages can be utilized to improve the performance by jointly making full use of the adaptive time allocation and energy allocation.

We compare the achievable throughput in wireless powered relaying networks with single relay and two relays in Figure 5, where both the relay selection and successive relaying protocols are considered in two relays networks. In order to guarantee that the consumed energy is the same and equal to 1 Joule per slot, the transmit powers of the source in single relay and relay selection schemes is $2P_s/1+\alpha$. One may reasily observe that the achievable throughput of the WPSR scheme is much larger than that of wireless powered relay network with either single relay or relay selection schemes, and in some case of α, the achievable throughput gain has been increased by about 1.8 times, which unveils that the throughput gain can be achieved by increasing the number of relays and designing the efficient SR protocol.

5.2. Adaptive WPBSR Scheduling Scheme. In this subsection, unless otherwise stated, we set $\lambda_k = 1$, $\phi_k = 0.1$, and $\mu_k = 15$ $V/0.9\eta L_0 \phi_k {d_{Sk}}^{-m}$ and evaluate the performance of the adaptive WPBSR schemes by varying V from 50 to 600.

Figure 6 presents the data buffer lengths of the relay $\mathscr{R}_2$ and the total data buffer length of both relays with different V, in which λ_2 is set to 0.6,1.0,1.4, respectively. A larger λ_2 results in the smaller data buffer lengths, which is consistent with the performance analysis in Section 5.3, and the average data buffer length tends to be linearly proportional to V, which complies with the analysis in (49). In addition, the maximal data buffer length at the relay $\mathscr{R}_2$ is just a litter larger than the parameter V/λ_2, which indicates that the instantaneous data buffer length is always bounded, which complies with Lemma 9.

In Figure 7, we present the instantaneous data buffer and energy storage length in the first 10000 time slots, respectively. Given $V = 250, \lambda_1 = 1, \lambda_2 = 1.4$, the instantaneous data buffer length of the first relay $\mathscr{R}_1$ fluctuates around the parameter V, and that of the second relay $\mathscr{R}_2$ is around $V/\lambda_2 = 178.5$. In addition, the maximal data buffer length is bounded and a litter larger than V/λ_k, which indicates that our proposed WPBSR scheme can guarantee the different bounds of both relays. Similarly, the instantaneous energy storage length is always less than the parameter ϕ_k, which complies with Lemma 9.

According to Figure 8, the achievable throughput first increases and then keeps sable with increasing V, and the transmission delay tends to be linearly proportional to V. The result is consistent with Theorem 10 and unveils that larger tolerable delay corresponds to a larger throughput improvement, and the adaptive WPBSR scheme can arbitrarily approach the optimal scheme by increasing the parameter V. In the adaptive WPBSR scheme, a larger V allows the relay caches more data for better information delivery scheduling and implies a larger temporal degree of freedom to adaptively allocate the time slot to three transmission mode. Of course, a larger data buffer length always results in a larger transmission delay.

5.3. Effect of the Relay Position Placement. Lastly, we investigate the achievable throughput of the proposed WPSR schemes in the cases of different relay position and compare them with that of the single relay scheme and relay selection scheme. In Figure 9, we evaluate the effect of different distance between the source and both relays by varying the distance from 5 to 20 meters. When the distance between the source and the relays increases, the achievable throughput of all transmission schemes decreases. On one hand, if d_{S1} increases, the achieved performance of the first hop is degraded due to the larger transmission distance. On the other hand, the harvested energy at the relays becomes smaller as well. Both factors cause the decreasing characteristic of the achievable throughput. Meanwhile, according to Figure 9, the achievable throughput of the WPBSR scheme is much larger than those of the single relay and relay selection schemes, which validates the significant throughput gain of the proposed wireless powered successive relaying schemes. In addition, for the adaptive WPBSR scheme, a larger V leads to a larger achievable throughput, and when V is large enough, the achieved throughput can arbitrarily approach the optimal throughput.

Figure 10 illustrates the achieved performance in the case of different θ, which is the angle between the lines from the source to the relay and from the source to the destination. θ affects not only the distance between the relays $d_{12} = d_{S1} \sin\theta$ but also the distance between the relays to the destination $d_{1D} = d_{2D} = \sqrt{d_{S1}^2 + d_{SD}^2 - 2d_{S1}d_{SD}\cos\theta}$. With a larger θ, both d_{12} and $d_{1D} = d_{2D}$ increase, and the achievable rate of the link from the source to the relay is enhanced due to the weaker inter-relay-interference (IRI), while that of the link from the relay to the destination is degraded due to the larger transmission distance. As shown in Figure 10, the achievable throughput is improved in the case of smaller θ, where the weaker IRI is the main factor, while in the case of larger θ, the larger transmission distance of second hop dominates the degraded performance.

6. Conclusion

In this paper, to enhance the spectral efficiency, we have proposed a wireless powered successive relaying protocol, where the successive relaying (SR) is utilized for the WIT. To reveal the potential of data buffers and energy storages, we have analyzed the achievable network throughput of WPSR scheme with and without data buffers and energy storages. When considering the data buffers at the relay, the data management strategy becomes buffer-and-forward, which always brings throughput gain. Meanwhile, with energy storages, the energy management strategy becomes harvest-store-use, and the energy allocation policy can be utilized, which enhances the performance of the links from the relay to the destination. To maximize the network throughput, the adaptive time and power allocation are jointly optimized to exploit the great potential of data buffers and energy storages, and an adaptive wireless powered buffer-aided successive relaying (WPBSR) scheme is proposed. The performance analysis and numerical results are presented to disclose that, the achievable throughput is able to arbitrarily approach the optimal scheme with limited cost of delay, while guaranteeing the finite and different lengths of both data buffers and energy storages at the relays. The extensions of the presented work to the power-splitting relaying (PSR), multiple relay networks, as well as more realistic system design issues (such as imperfect/outdate CSIs) can be explored in the next step work.

Appendix

A. Proof of Proposition 1

All channels are assumed to be independent Rayleigh fading. Define $x_1 = |h_{S1}(t)|^2, x_2 = |h_{S2}(t)|^2|h_{12}(t)|^2, x_3 = |h_{S1}(t)^2|h_{1D}(t)|^2$, then, we have the PDFs of x_1, x_2, x_3 as $f_1(x_1) = 1/\Omega_{S1} \exp(-x_1/\Omega_{S1}), f_2(x_2) = 2/\Omega_{S2}\Omega_{12}K_0(2\sqrt{x_2/\Omega_{S2}\Omega_{12}}), f_3(x_3) = 2/\Omega_{S1}\Omega_{1D}K_0(2\sqrt{x_3/\Omega_{S1}\Omega_{1D}})$. Meanwhile, the SNRs of the links $\mathcal{SR}_1$ and $\mathcal{R}_1\mathcal{D}$ can be rewritten as $\gamma_{S1}(t) = P_s x_1/\sigma_1^2 + \kappa\eta P_s x_2$ and $\gamma_{1D}(t) = \kappa\eta P_s x_3/\sigma_d^2$, where $\kappa = 2\alpha/1-\alpha$. To derive the CDF of $\gamma_{S1}(t)$, we have

$$\begin{aligned} F_{\gamma_{S1}}(\gamma) &= 1 - \Pr\left(x_1 > \frac{\gamma\left(\sigma_1^2 + \kappa\eta P_s x_2\right)}{P_s}\right) \\ &= 1 - \int_0^\infty \exp\left(-\frac{\gamma\left(\sigma_1^2 + \kappa\eta P_s x_2\right)}{\Omega_{S1}P_s}\right) f_2(x_2)x_2 \\ &= 1 - \frac{\exp\left(-\left(\sigma_1^2/\Omega_{S1}P_s\right)\gamma\right)\exp\left(1/2(\Omega_{S1}/\kappa\eta\gamma\Omega_{S2}\Omega_{12})\right)}{\sqrt{\kappa\eta\gamma\Omega_{S2}\Omega_{12}/\Omega_{S1}}} \\ &\quad \cdot W_{-1/2,0}\left(\frac{\Omega_{S1}}{\kappa\eta\gamma\Omega_{S2}\Omega_{12}}\right), \end{aligned} \tag{A.1}$$

where the computation detail is referred to [52]. And the CDF of $\gamma_{1D}(t)$ is given as

$$\begin{aligned} F_{\gamma_{1D}}(\gamma) &= \Pr\left(x_3 \le \frac{\sigma_d^2\gamma}{\kappa\eta P_s}\right) \\ &= 1 - 2\sqrt{\frac{\sigma_d^2\gamma}{\kappa\eta P_s\Omega_{S1}\Omega_{1D}}}K_1\left(2\sqrt{\frac{\sigma_d^2\gamma}{\kappa\eta P_s\Omega_{S1}\Omega_{1D}}}\right). \end{aligned} \tag{A.2}$$

The similar procedure can be applied to compute the CDFs of the SNRs $\gamma_{S2}(t)$ and $\gamma_{2D}(t)$.

B. Proof of Equations (14) and (15)

Given the same symbol definition of x_1, x_2, x_3 in Appendix A, the E2E SNR $\gamma_{S1D}(t)$ can be rewritten as $\gamma_{S1D}(t) = x_1 z = x_1 \min\{Ps/\sigma_1^2 + \kappa\eta P_s x_2, \kappa\eta Psx_3/\sigma_d^2\}$. Then, we have the CDF of z as

$$\begin{aligned} F_Z(z) &= 1 - \Pr\left(\frac{Ps}{\sigma_1^2 + \kappa\eta P_s x_2} > z\right)\Pr\left(\frac{\kappa\eta Psx_3}{\sigma_d^2} > z\right) \\ &= 1 - \left[1 - 2\sqrt{\frac{P_s/z - \sigma_1^2}{\kappa\eta P_s \Omega_{S1}\Omega_{12}}}K_1\left(2\sqrt{\frac{P_s/z - \sigma_1^2}{\kappa\eta P_s\Omega_{S1}\Omega_{12}}}\right)\right]\exp \\ &\quad \cdot \left(-\frac{z\sigma_d^2}{\kappa\eta P_s \Omega_{1D}}\right), \end{aligned} \tag{B.1}$$

and the CDF of $\gamma_{S1D}(t)$ can be given by

$$\begin{aligned} F_{\gamma_{S1D}}(\gamma) &= \Pr\left(0 \le x_1 \le +\infty, 0 \le z \le \frac{P_s}{\sigma_1^2}\right) \\ &\quad + \Pr\left(\frac{\gamma\sigma_1^2}{P_s} \le x_1 \le +\infty, 0 \le z \le \frac{\gamma}{x_1}\right) \\ &= 1 - \int_{\gamma\sigma_1^2/P_s}^{+\infty} \frac{1}{\Omega_{S1}} \exp\left(-\frac{x_1}{\Omega_{S1}} - \frac{\gamma\sigma_d^2}{\kappa\eta P_s\Omega_{1D}x_1}\right) \\ &\quad \cdot \left[1 - 2\sqrt{\frac{P_s\gamma/x_1 - \sigma_1^2}{\kappa\eta P_s\Omega_{S1}\Omega_{12}}}K_1\left(2\sqrt{\frac{P_s\gamma/x_1 - \sigma_1^2}{\kappa\eta P_s\Omega_{S1}\Omega_{12}}}\right)\right]x_1 \\ &= 1 - \int_0^{+\infty} \frac{\gamma}{P_s\Omega_{S1}} \exp\left(-\frac{\gamma(x+\sigma_1^2)}{P_s\Omega_{S1}} - \frac{\sigma_d^2}{\kappa\eta\Omega_{1D}(x+\sigma_1^2)}\right) \\ &\quad \cdot \left[1 - 2\sqrt{\frac{x}{\kappa\eta \cdot P_s\Omega_{S1}\Omega_{12}}}K_1\left(2\sqrt{\frac{x}{\kappa\eta P_s\Omega_{S1}\Omega_{12}}}\right)\right]x. \end{aligned} \tag{B.2}$$

By careful observation, the SNRs $\gamma_{S2}(t-1)$ and $\gamma_{2D}(t)$ are independent, thus, we can easily derive the E2E SNR γ_{S2D} as $F_{\gamma_{S2D}}(\gamma) = 1 - [1 - F_{\gamma_{S2}}(\gamma)][1 - F_{\gamma_{2D}}(\gamma)]$.

C. Proof of Theorem 10

There always exists a stationary randomized scheme independent of buffer and energy state for (34), which satisfies

$$\mathbb{E}\left[\sum_k R_{Sk}^*(t)\middle|\Theta(t)\right] = \mathbb{E}\left[\sum_k R_{Sk}^*(t)\right] = \Psi(\varepsilon), \tag{C.1}$$

$$\mathbb{E}[R_{Sk}^*(t) - R_{kD}^*(t)|\Theta(t)] = \mathbb{E}[R_{Sk}^*(t) - R_{kD}^*(t)] \le -\varepsilon, \tag{C.2}$$

$$\mathbb{E}\left[e_k^{c*}(t) - e_k^{h*}(t)\middle|\Theta(t)\right] = \mathbb{E}\left[e_k^{c*}(t) - e_k^{h*}(t)\right] = 0. \tag{C.3}$$

Here, we follow the similar proof in [55]. The proposed adaptive WPSR scheme is to minimize the right hand side of (40) over all fading scenarios and possible policies. With (C.1), (C.2), and (C.3), it yields

$$\Delta(\Theta(t)) - V\sum_k \mathbb{E}[R_{Sk}(t)|\Theta(t)] \le B - V\Psi(\varepsilon) - \varepsilon\sum_k \lambda_k Q_k(t). \tag{C.4}$$

Taking expectation and using telescoping sums in the above inequality, we get

$$\begin{aligned} &\mathbb{E}[L(\Theta(t))] - \mathbb{E}[L(\Theta(0))] - V\sum_{\tau=0}^{t-1}\mathbb{E}\left[\sum_k R_{Sk}(\tau)\right] \\ &\le [B - V\Psi(\varepsilon)]\cdot t - \varepsilon\sum_{\tau=0}^{t-1}\mathbb{E}\left[\sum_k \lambda_k Q_k(\tau)\right]. \end{aligned} \tag{C.5}$$

(1) Based on Lyapunov function, we can get the following inequality by rearranging (C.5)

$$\begin{aligned} \mathbb{E}\left[\frac{\mu_k}{2}[E_k(t)]^2\right] &\le [B - V\Psi(\varepsilon)]\cdot t + \mathbb{E}[L(\Theta(0))] \\ &\quad + V\sum_{\tau=0}^{t-1}\mathbb{E}\left[\sum_k R_{Sk}(\tau)\right]. \end{aligned} \tag{C.6}$$

Due to the fact that $[\mathbb{E}\{|E_k(t)|\}]^2 \le \mathbb{E}\{[E_k(t)]^2\}$ and $\mathbb{E}[\sum_{k\in\{1,2\}} R_{Sk}(\tau)]$ are not larger than the optimal achievable throughput R^{opt}, thus, we have

$$\mathbb{E}[|E_k(t)|] \le \sqrt{\frac{2t[B - V\Psi(\varepsilon) + VR^{\text{opt}}] + 2\mathbb{E}[L(\Theta(0))]}{\mu_k}}. \tag{C.7}$$

Dividing (C.7) by t and taking a limit as $t \longrightarrow \infty$ results in $\lim_{t\longrightarrow\infty}\mathbb{E}[|E_k(t)|]/t = 0$. Hence, the energy queue $E_k(t)$ is mean rate stable, similar proof can be applied to buffer queue $Q_k(t)$. Thus, the constraints (32) and (33) in (34) can be guaranteed.

(2) Dividing (C.5) with Vt, rearranging items and using the fact that $\mathbb{E}[L(\Theta(t))] \ge 0$ and $Q_k(t) \ge 0$, we may have

$$\frac{1}{t}\sum_{\tau=0}^{t-1}\mathbb{E}\left[\sum_k R_{Sk}(\tau)\right] \ge \Psi(\varepsilon) - \frac{B}{V} - \frac{\mathbb{E}[L(\Theta(0))]}{Vt}. \tag{C.8}$$

Taking a limit as $t \longrightarrow \infty$ and $\Psi(\varepsilon) \longrightarrow R^{\text{opt}}$ as $\varepsilon \longrightarrow 0$, we can derive the lower bound of achievable throughput. Similarly, we can rewrite (C.5) as

$$\frac{1}{t}\sum_{\tau=0}^{t-1}\mathbb{E}\left[\sum_{k}\lambda_k Q_k(\tau)\right] \leq \frac{B-V\Psi(\varepsilon)}{\varepsilon} + \frac{V}{\varepsilon t}\sum_{\tau=0}^{t-1}\mathbb{E}\left[\sum_{k}R_{Sk}(\tau)\right] + \frac{\mathbb{E}[L(\Theta(0))]}{\varepsilon t}. \tag{C.9}$$

Taking a limit as $t \longrightarrow \infty$, the upper bound of average buffer size can be derived.

Data Availability

No data were used to support this study.

Conflicts of Interest

The authors declare that they have no conflicts of interest.

Acknowledgments

The work of Yong Liu was supported in part by the National Natural Science Foundation of China under Grant 61901180 and Grant 61771406. The work of Qingchun Chen was supported in part by the National Natural Science Foundation of China under Grant 61771406 and Grant 61971360, and in part by the Lingnan Yingjie Project by Guangzhou Municipal Government. The work of Lin X. Cai was supported in part by the National Science Foundation under Grant ECCS-1554576.

References

[1] X. Lu, P. Wang, D. Niyato, D. Kim, and Z. Han, "Wireless networks with rf energy harvesting: a contemporary survey," *IEEE Communications Surveys & Tutorials*, vol. 17, no. 2, pp. 757–789, 2015.

[2] R. Zhang and C. Ho, "MIMO broadcasting for simultaneous wireless information and power transfer," *IEEE Transactions on Wireless Communications*, vol. 12, no. 5, pp. 1989–2001, 2013.

[3] X. Zhou, R. Zhang, and C. Ho, "Wireless information and power transfer: architecture design and rate-energy tradeoff," *IEEE Transactions on Communications*, vol. 61, no. 11, pp. 4754–4767, 2013.

[4] C. Liu, M. Maso, S. Lakshminarayana, C. Lee, and T. Quek, "Simultaneous wireless information and power transfer under different csi acquisition schemes," *IEEE Transactions on Wireless Communications*, vol. 14, no. 4, pp. 1911–1926, 2015.

[5] T. D. P. Perera, D. Jayakody, S. K. Sharma, S. Chatzinotas, and J. Y. Li, "Simultaneous wireless information and power transfer (swipt): recent advances and future challenges," *IEEE Communications Surveys & Tutorials*, vol. 20, no. 1, pp. 264–302, 2018.

[6] N. Zlatanov, A. Ikhlef, T. Islam, and R. Schober, "Buffer-aided cooperative communications: opportunities and challenges," *IEEE Communications Magazine*, vol. 52, no. 4, pp. 146–153, 2014.

[7] N. Nomikos, T. Charalambous, D. Vouyioukas, and G. Karagiannidis, "When buffer-aided relaying meets full duplex and noma," *IEEE Wireless Communications*, vol. 28, no. 1, pp. 68–73, 2021.

[8] R. Berry and R. Gallager, "Communication over fading channels with delay constraints," *IEEE Transactions on Information Theory*, vol. 48, no. 5, pp. 1135–1149, 2002.

[9] B. Xia, Y. Fan, J. Thompson, and H. Poor, "Buffering in a three-node relay network," *IEEE Transactions on Wireless Communications*, vol. 7, no. 11, pp. 4492–4496, 2008.

[10] N. Zlatanov, R. Schober, and P. Popovski, "Buffer-aided relaying with adaptive link selection," *IEEE Journal on Selected Areas in Communications*, vol. 31, no. 8, pp. 1530–1542, 2013.

[11] A. Nasir, X. Zhou, S. Durrani, and R. Kennedy, "Relaying protocols for wireless energy harvesting and information processing," *IEEE Transactions on Wireless Communications*, vol. 12, no. 7, pp. 3622–3636, 2013.

[12] A. A. Nasir, X. Zhou, S. Durrani, and R. A. Kennedy, "Throughput and ergodic capacity of wireless energy harvesting based df relaying network," in *2014 IEEE International Conference on Communications (ICC)*, pp. 4066–4071, Sydney, NSW, Australia, 2014.

[13] Y. Gu and S. Aissa, "Rf-based energy harvesting in decode-and-forward relaying systems: ergodic and outage capacities," *IEEE Transactions on Wireless Communications*, vol. 14, no. 11, pp. 6425–6434, 2015.

[14] M. Ju, K.-M. Kang, K.-S. Hwang, and C. Jeong, "Maximum transmission rate of psr/tsr protocols in wireless energy harvesting df-based relay networks," *IEEE Journal on Selected Areas in Communications*, vol. 33, no. 12, pp. 2701–2717, 2015.

[15] B. Lyu, T. Qi, H. Guo, and Z. Yang, "Throughput maximization in full-duplex dual-hop wireless powered communication networks," *IEEE Access*, vol. 7, pp. 158584–158593, 2019.

[16] I. Krikidis, "Relay selection in wireless powered cooperative networks with energy storage," *IEEE Journal on Selected Areas in Communications*, vol. 33, no. 12, pp. 2596–2610, 2015.

[17] Y. Liu, "Wireless information and power transfer for multirelay-assisted cooperative communication," *IEEE Communications Letters*, vol. 20, no. 4, pp. 784–787, 2016.

[18] Y. Huang and B. Clerckx, "Relaying strategies for wireless-powered mimo relay networks," *IEEE Transactions on Wireless Communications*, vol. 15, no. 9, pp. 6033–6047, 2016.

[19] A. G. Onalan, E. D. Salik, and S. Coleri, "Relay selection, scheduling, and power control in wireless-powered cooperative communication networks," *IEEE Transactions on Wireless Communications*, vol. 19, no. 11, pp. 7181–7195, 2020.

[20] O. Messadi, A. Sali, V. Khodamoradi et al., "Optimal relay selection scheme with multiantenna power beacon for wireless-powered cooperation communication networks," *Sensors*, vol. 21, no. 1, p. 147, 2021.

[21] B. Picano and R. Fantacci, "An intelligent radio buffer-aided relaying scheme with adaptive link selection," *IEEE Transactions on Vehicular Technology*, vol. 70, no. 4, pp. 3677–3684, 2021.

[22] N. Zlatanov, V. Jamali, and R. Schober, "Achievable rates for the fading half-duplex single relay selection network using buffer-aided relaying," *IEEE Transactions on Wireless Communications*, vol. 14, no. 8, pp. 4494–4507, 2015.

[23] N. Nomikos, E. T. Michailidis, P. Trakadas, D. Vouyioukas, T. V. Zahariadis, and I. Krikidis, "Flex-noma: exploiting buffer-aided relay selection for massive connectivity in the 5g uplink," *IEEE Access*, vol. 7, pp. 88743–88755, 2019.

[24] S. El-Zahr and C. Abou-Rjeily, "Threshold based relay selection for buffer-aided cooperative relaying systems," *IEEE*

Transactions on Wireless Communications, vol. 20, no. 9, pp. 6210–6223, 2021.

[25] S. Luo, G. Yang, and K. Teh, "Throughput of wireless-powered relaying systems with buffer-aided hybrid relay," *IEEE Transactions on Wireless Communications*, vol. 15, no. 7, pp. 4790–4801, 2016.

[26] D. Bapatla and S. Prakriya, "Performance of two-hop links with an energy buffer-aided iot source and a data buffer-aided relay," *IEEE Internet of Things Journal*, vol. 8, no. 6, pp. 5045–5061, 2021.

[27] P. Huynh, K. T. Phan, B. Liu, and R. Ross, "Throughput analysis of buffer-aided decode-and-forward wireless relaying with rf energy harvesting," *Sensors*, vol. 20, no. 4, p. 1222, 2020.

[28] C.-H. Lin and K.-H. S. Liu, "Relay selection for energy-harvesting relays with finite data buffer and energy storage," *IEEE Internet of Things Journal*, vol. 8, no. 14, pp. 11249–11259, 2021.

[29] S. Luo and K. Teh, "Throughput maximization for wireless-powered buffer-aided cooperative relaying systems," *IEEE Transactions on Communications*, vol. 64, no. 6, pp. 2299–2310, 2016.

[30] X. Lan, Y. Zhang, Q. Chen, and L. X. Cai, "Energy efficient buffer-aided transmission scheme in wireless powered cooperative noma relay network," *IEEE Transactions on Communications*, vol. 68, no. 3, pp. 1432–1447, 2020.

[31] J. Ren, X. Lei, P. D. Diamantoulakis, Q. Chen, and G. K. Karagiannidis, "Buffer-aided secure relay networks with swipt," *IEEE Transactions on Vehicular Technology*, vol. 69, no. 6, pp. 6485–6499, 2020.

[32] B. Rankov and A. Wittneben, "Spectral efficient protocols for half-duplex fading relay channels," *IEEE Journal on Selected Areas in Communications*, vol. 25, no. 2, pp. 379–389, 2007.

[33] C. Zhong, H. Suraweera, G. Zheng, I. Krikidis, and Z. Zhang, "Wireless information and power transfer with full duplex relaying," *IEEE Transactions on Communications*, vol. 62, no. 10, pp. 3447–3461, 2014.

[34] Y. Zeng and R. Zhang, "Full-duplex wireless-powered relay with self-energy recycling," *IEEE Wireless Communications Letters*, vol. 4, no. 2, pp. 201–204, 2015.

[35] M. Mohammadi, B. K. Chalise, H. Suraweera, C. Zhong, G. Zheng, and I. Krikidis, "Throughput analysis and optimization of wireless-powered multiple antenna full-duplex relay systems," *IEEE Transactions on Communications*, vol. 64, no. 4, pp. 1769–1785, 2016.

[36] M. M. Razlighi and N. Zlatanov, "Buffer-aided relaying for the two-hop full-duplex relay channel with self-interference," *IEEE Transactions on Wireless Communications*, vol. 17, no. 1, pp. 477–491, 2018.

[37] N. Nomikos, T. Charalambous, D. Vouyioukas, R. Wichman, and G. K. Karagiannidis, "Integrating broadcasting and noma in full-duplex buffer-aided opportunistic relay networks," *IEEE Transactions on Vehicular Technology*, vol. 69, no. 8, pp. 9157–9162, 2020.

[38] R. Zhang, "On achievable rates of two-path successive relaying," *IEEE Transactions on Communications*, vol. 57, no. 10, pp. 2914–2917, 2009.

[39] Y. Hu, C. Xu, Y. Zhang, and L. Ping, "Joint power and rate allocation for df two-path relay systems," *IEEE Wireless Communications Letters*, vol. 5, no. 6, pp. 620–623, 2016.

[40] A. V. Mampilly and S. Bhashyam, "Successive relaying for two-hop two-destination multicarrier relay channels," *IEEE Communications Letters*, vol. 24, no. 3, pp. 685–689, 2020.

[41] N. Nomikos, T. Charalambous, I. Krikidis, D. N. Skoutas, D. Vouyioukas, and M. Johansson, "A buffer-aided successive opportunistic relay selection scheme with power adaptation and inter-relay interference cancellation for cooperative diversity systems," *IEEE Transactions on Communications*, vol. 63, no. 5, pp. 1623–1634, 2015.

[42] O. Orhan and E. Erkip, "Energy harvesting two-hop communication networks," *IEEE Journal on Selected Areas in Communications*, vol. 33, no. 12, pp. 2658–2670, 2015.

[43] C. Zhai, L. Zheng, P. Lan, and H. Chen, "Wireless powered cooperative communication using two relays: protocol design and performance analysis," *IEEE Transactions on Vehicular Technology*, vol. 67, no. 4, pp. 3598–3611, 2018.

[44] M. Oiwa and S. Sugiura, "Generalized virtual full-duplex relaying protocol based on buffer-aided half-duplex relay nodes," in *GLOBECOM 2017 - 2017 IEEE Global Communications Conference*, pp. 1–6, Singapore, 2017.

[45] B. R. Manoj, R. K. Mallik, M. R. Bhatnagar, and S. Gautam, "Virtual full-duplex relaying in multi-hop df cooperative networks using half-duplex relays with buffers," *IET Communications*, vol. 13, no. 5, pp. 489–495, 2019.

[46] A. K. Shukla, B. R. Manoj, and M. R. Bhatnagar, "Virtual full-duplex relaying in a buffer-aided multi-hop cooperative network," in *2020 International Conference on Signal Processing and Communications (SPCOM)*, pp. 1–5, 2020.

[47] G. Srirutchataboon, J. Kochi, and S. Sugiura, "Performance analysis of hybrid buffer-aided cooperative protocol based on half-duplex and virtual full-duplex relay selections," *IEEE Open Journal of the Communications Society*, vol. 2, pp. 1862–1873, 2021.

[48] N. Nomikos, T. Charalambous, N. Pappas, D. Vouyioukas, and R. Wichman, "Lola4sor: a low-latency algorithm for successive opportunistic relaying," in *IEEE INFOCOM 2019 - IEEE Conference on Computer Communications Workshops (INFOCOM WKSHPS)*, pp. 1–6, Paris, France, 2019.

[49] N. Nomikos, T. Charalambous, N. Pappas, D. Vouyioukas, and R. Wichman, "Lola4sor: leveraging successive transmissions for low-latency buffer-aided opportunistic relay networks," *IEEE Open Journal of the Communications Society*, vol. 2, pp. 1041–1054, 2021.

[50] S. Gupta, R. Zhang, and L. Hanzo, "Throughput maximization for a buffer-aided successive relaying network employing energy harvesting," *IEEE Transactions on Vehicular Technology*, vol. 65, no. 8, pp. 6758–6765, 2016.

[51] G. Shabbir, J. Ahmad, W. Raza et al., "Buffer-aided successive relay selection scheme for energy harvesting iot networks," *IEEE Access*, vol. 7, pp. 36246–36258, 2019.

[52] V. Jamali, N. Zlatanov, A. Ikhlef, and R. Schober, "Achievable rate region of the bidirectional buffer-aided relay channel with block fading," *IEEE Transactions on Information Theory*, vol. 60, no. 11, pp. 7090–7111, 2014.

[53] A. Alsharoa, H. Ghazzai, A. Kamal, and A. Kadri, "Wireless rf-based energy harvesting for two-way relaying systems," in *2016 IEEE Wireless Communications and Networking Conference*, pp. 1–6, Doha, Qatar, 2016.

[54] I. S. Gradshteyn and I. M. Ryzhik, *Table of Integrals, Series, and Products*, Academic Press, 2007.

[55] G. Zheng, H. Suraweera, and I. Krikidis, "Optimization of hybrid cache placement for collaborative relaying," *IEEE Communications Letters*, vol. 21, no. 2, pp. 442–445, 2017.

[56] Y. Zhang, S. He, and J. Chen, "Near optimal data gathering in rechargeable sensor networks with a mobile sink," *IEEE Transactions on Mobile Computing*, vol. 16, no. 6, pp. 1718–1729, 2017.

[57] M. J. Neely, "Stochastic network optimization with application to communication and queueing systems," *Synthesis Lectures on Communication Networks*, vol. 3, no. 1, pp. 1–211, 2010.

[58] A. Yuille and A. Rangarajan, "The concave-convex procedure," *Neural Computation*, vol. 15, no. 4, pp. 915–936, 2003.

[59] H. Tuy, *D.c. optimization: Theory, methods and algorithms*, 1995.

[60] N. Proskurin, "On the cubic L-function," *St Petersburg Mathematical Journal*, vol. 24, no. 2, pp. 353–370, 2013.